DEVELOPMENT OF A VERTICALLY LANDED ROCKET DESIGN CHALLENGE FOR EXPANDING THE PIPELINE AND ENHANCING EDUCATION OF STUDENTS PURSUING CAREERS IN SPACE

BY

COURTNEY TROM

THESIS

Submitted in partial fulfillment of the requirements
for the degree of Master of Science in Aerospace Engineering
in the Graduate College of the
University of Illinois Urbana-Champaign, 2022

Urbana, Illinois

Adviser:

Clinical Associate Professor Michael Lembeck

ABSTRACT

As part of the DOD funded grant, "*Expanding the Pipeline and Enhancing Education of Students Pursuing Careers in Space*," a design challenge was formulated to attract students to careers in aerospace by exposing them to an integrated set of educational resources. As part of the program undertaken to achieve this objective, a student aerospace design challenge was formulated, focused on vertically landing a previously lofted model rocket, hereafter called the vertically landed rocket (VLR). This thesis describes the processes, analyses, and testing undertaken to satisfy this objective.

A modified model rocket was developed to be carried aloft by an unmanned aerial vehicle (UAV), released from the UAV, and allowed to descend under the control of a gimballed solid rocket motor to an upright landing. To accomplish this, the rocket incorporated an avionics package, including software and sensors to track and monitor orientation, and a pair of servos to gimbal the model rocket motor slowing the descending rocket to a landing on an extended set of legs mounted circumferentially around the rocket base. This concept is designed to be packaged as a project with assembly instructions and educational videos that student teams could work on in either a moderated classroom or at home in a self-paced environment.

To validate design choices, a series of verification tests were conducted. A simulation has been created to find optimal flight parameters and predict the VLR's performance. The motor's thrust output and performance had been tested and verified and fed back into the simulation to refine parameters and performance predictions. A closed loop test was conducted to examine the effect sensor noise would have on the rocket and to verify even in its presence, that the VLR could successfully land. A thrust test stand was created and tested on to verify that the avionics

and power were capable of igniting the motor and maintaining control over the gimbal while remaining powered and in contact with the ground station. A mode verification test was conducted to verify the software's capability of stepping through the different modes of flight and to ensure data collection and unhindered connection with the ground station. Finally, a series of drop tests were conducted to verify the passive stability of the rocket and to verify the landing legs' ability to accept and disperse energy of landing. This series of tests validated the design choices and led to the approval to test powered VLRs.

ACKNOWLEDGMENTS

I would like to first thank my advisor Dr. Michael Lembeck for the opportunity to work in the Laboratory for Advanced Space Systems at Illinois (LASSI). Under his guidance and work, LASSI has become a successful and welcoming lab and being a part of this group has provided me with immeasurable support and help that allowed me to learn, explore, and grow throughout my research. I would also like to thank Dr. Jason Merret for his continued help and support with testing.

I would like to thank the National Defense Education Program (NDEP) for Science, Technology, Engineering, and Mathematics (STEM) Education, Outreach, and Workforce Initiative Programs. Through them this research project was funded and brought to life.

This project would not have been manageable alone, and I want to thank my teammates who dedicated themselves to this project with me: David Gable, Qi Lim, Chris Young, Nate Madell, James Helmich, Hongrui Zhou, and everyone else who contributed. I would also like to thank LASSI members Logan Power and Rick Eason for their support and endless patience. Additionally, I want to thank our Laboratory Manager, Murphy Stratton, for her aid in procuring components for this project.

To my family, thank you for believing in me and cheering me on. Your love and support helped me keep progressing. To my closest friends, Jacob Kraft, Aldo Montagner, and Oscar Ortiz, thank you for reminding me to enjoy my time and take breaks away from work. Special thanks to Jacob and Fenyx for being my sanity and partners in crime.

To Fenyx, for your unconditional love.

TABLE OF CONTENTS

CHAPTER 1: INTRODUCTION

1.1 PROJECT OBJECTIVE

A principal objective of the Department of Defense funded grant, "*Expanding the Pipeline and Enhancing Education of Students Pursuing Careers in Space*," is to attract students to careers in aerospace by exposing them to an integrated set of educational resources implemented strategically in undergraduate classrooms, K-12, classrooms, outreach events, and workshops. As part of the program undertaken to achieve this objective, in a collaboration between the University of Illinois at Urbana-Champaign (UIUC) and Southern Illinois University at Edwardsville (SIUE), a student aerospace design challenge was formulated, focused on vertically landing a previously lofted model rocket, hereafter called the vertically landed rocket (VLR) [1]. This thesis describes the processes, analyses, and testing undertaken to satisfy this objective.

The idea for the challenge was originally conceptualized in the UIUC Aerospace Engineering Department's two semester capstone Aerospace Design class sequence. Modified model rockets were developed by teams of students, to be carried aloft by an unmanned aerial vehicle (UAV), released from the UAV, and allowed to descend under the control of a gimballed solid rocket motor to an upright landing (Figure 1). To accomplish this, the rockets incorporated an avionics package, including software and sensors to track and monitor orientation, and a pair of servos to gimbal the model rocket motor slowing the descending rocket to a landing on an extended set of legs mounted circumferentially around the rocket base.

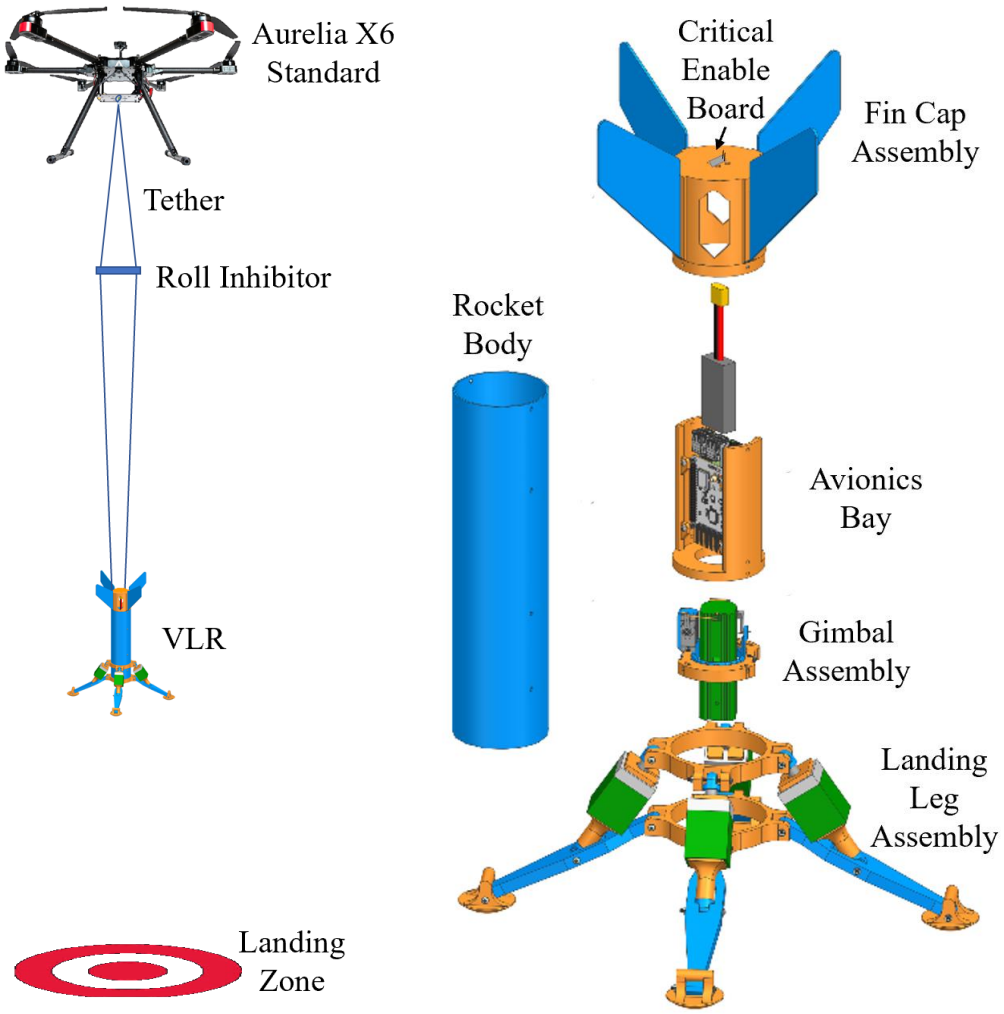

Figure 1: Vertically Landed Rocket Model

For the DoD grant, it was desired to package this concept into a project with assembly instructions and educational videos that student teams could work on in either a moderated classroom or at home in a self-paced environment. This is done by creating an integrated set of educational resources focused on space, specifically: (1) Massive Online Open Courses (MOOCs) containing videos and handbooks created by space experts; (2) hands-on kits with space-relevant sensors, avionics, and robotics; ultimately packaged into (3) an undergraduate student design challenge to vertically landing a model rocket. Each team selects its own UAV release height, solid rocket motor ignition time, and the rocket motor itself to land intact when

dropped from the UAV. UIUC/SIUE arranges the logistics for the teams to come together at designated sites to engage in a competition with their models. The competition awards participating teams for making successful parameter choices allowing them to vertically land their rockets.

The project supports participants going through each MOOC associated with the project. Students gain an understanding of the components and processes that go into the VLR. The MOOCs also show the real-life application to this project to garner interest in pursuing a career in space. After completing the courses, the students have the opportunity to assemble and test the VLR. From the MOOCs, they gain an understanding of the hardware that is involved and how the data collected is used, they also learn about critical parameters and how they affect the VLR's performance. Simulation software is provided for students to change the drop height, ignition delay, gimbal control gains, and motor selection so that they can see the effect each parameter has on the descent and landing.

The landing challenge is formulated as a competition between undergraduate teams who have completed the same coursework. Following the competition, students are able to analyze the data from the landing to see how the VLR behaved and to see how much it varied from the expected performance. Participants rate their experiences after going through the MOOCs and the competition. To evaluate the effectiveness of these educational resources, surveys are conducted before and after the project is completed assessing the student's knowledge gained and their interest in pursuing a career in aerospace.

Several UIUC students, including David Gable, Qi Lim, Nate Madell, James Helmich, and Chris Young, participated in the formulation of this challenge. Responsibilities were

assigned for the structural package, the avionics and software package, modeling and analysis, competition day logistics, and program feedback and evaluation. This thesis focuses on the overarching research and development of the VLR concept, with particular focus on the avionics and software package, but also provides relevant details from the other packages to provide context for the presented work.

1.2 BACKGROUND

The inspiration for this challenge is rooted in the industry's efforts to more efficiently provide access to space. Launch vehicles have mostly been expendable, transporting payloads into orbit and being disposed of after a single use. Akin to throwing away an airplane after a single flight, this drives the cost of access to space significantly. A different design philosophy was required to develop the technologies needed to introduce reusability into launch vehicle designs.

Historically, the first vertically landed space vehicle from the United States was not a launch vehicle but the Surveyor series of lunar soft landers. Followed later by the Apollo Lunar Modules, both vehicles descended from altitude to the lunar surface for a controlled upright landing.

Inherent in the quest for launch vehicle reusability is the requirement for a rocket to repeatedly take-off and land. The first attempt at realizing this objective was embodied in the Delta Clipper Experimental, DC-X, which was designed to demonstrate vertical take-off and landing capabilities and was built as a 1/3 scale prototype. This rocket took off vertically like standard rockets, but then performed a controlled return to land vertically on the ground. This was done using attitude control thrusters and retrorockets to control the descent. After reaching

peak altitude, the DC-X entered the atmosphere nose-first and then rolled around during the descent to touch down on landing struts. The main purpose of this was to demonstrate reusability and be able to take off and land from the same location [2]. DC-X was flown several times between 1993 and 1996, before succumbing to a landing failure that destroyed the test article.

The Rotary Rocket Roton was a rocket that would takeoff vertically like a conventional rocket powered by a novel rotary engine burning liquid oxygen and jet fuel. The Roton was designed to lift-off under command of a human crew and fly to orbit from the launch site. Once its payload was deployed, the Roton returned to Earth and deployed a nose-mounted rotor. The rotor recovery system was lightweight and was designed to provide a slow, pilot-controlled approach to the landing site. The rotor system consisted of a set of four rotor blades, a rotor hub, and a nose cap. Before re-entry, the blades were deployed and angled upward away from the nose. During the hypersonic and supersonic phases of flight, the base of the vehicle produced most of the drag while the rotor remained windmilling behind the vehicle, stabilizing it until it reached subsonic speed. The rotor would then be spun up and the blades entered a helicopter-style autorotation flight mode. While in this mode, the Roton was able to glide with the pilot's direction to a precision landing point. The vehicle's rotors would be equipped with tip rockets so that the Roton could touchdown softly under rotor power. An Atmospheric Test Vehicle flew three successful test flights in 1999 [3].

The SpaceX Falcon 9 is a reusable, two-stage rocket designed for the reliable and safe transport of people and payloads into Earth orbit and beyond. It first flew in 2010. The boosters incorporate high precision GPS, gyroscopes, and accelerometers at both top and bottom ends to precisely interpolate the booster orientation, position, and velocity. The boosters also contain a

number of strain gauges that monitor forces on the structure at crucial locations. This data is used to calculate the booster's orientation and flight trajectory. By comparing the past position vector to the desired course, the latest navigation error is calculated. The flight path is then optimized, controlled by thrust vectoring, grid fin positioning, and cold gas thruster pulses. At apogee, a boost-back burn flips the first stage end-for-end. The burn reverses horizontal velocity to return to land near the launch site or, to a drone-ship for an at-sea landing [4]. Reusing the boosters allows SpaceX to re-fly the most expensive parts of the rocket, which in turn drives down the cost of space access.

The Rocket Lab Neutron is a new concept consisting of two booster stages. The first stage features an integrated four-blade payload fairing that opens in orbit to release the second stage carrying the payload. The first stage is designed to be fully reusable. The second stage that delivers payloads to their target orbits is not designed to be reused [5]. The Neutron operates similarly to an aircraft in that it will require minimum amount of servicing between flights.

Blue Origin's New Shepard space tourism booster is a fully reusable vertical takeoff, vertical landing rocket. The system has a capsule atop the booster that is launched on a suborbital trajectory before the booster returns and performs an autonomously controlled rocket-powered vertical landing. The capsule itself returns under parachutes to a desert landing. The booster uses fins and aero-brakes to slow and control the descent before firing its single BE-3 rocket engine to slow to a vertical touchdown [6].

Blue Origin's New Glenn is a two-stage heavy-lift launch vehicle that is designed to have the capacity to carry payloads and people to the earth's orbit and beyond. The New Glenn launch

vehicle features a fully reusable first-stage booster. The vehicle's two wing-like strakes aid in providing lift and cross-range for the first stage during the descent along with four forward actuating fins. The first stage lands on a moving ship on six hydraulically actuated legs [7].

CHAPTER 2: VERTICALLY LANDED ROCKET

As a result of findings from the research of similar successful technical student engagement programs [8], a hands-on project with guidance from mentors and videos was formulated, culminating in the design of a competition that provides inspiration and guidance for pursuing a career in aerospace engineering. The key element in this approach is the development of the VLR itself. The rocket had to be designed in such a way that it was understandable to the students who would be assembling the kits, and highly interactive and accessible to them as well. This led to the decision to use off the shelf parts when available, as well as 3D printed parts for unique items. A series of videos are being created to walk the students through the development of the VLR and the decision making process behind its design features. The VLR competition allows students to uniquely set performance parameters for each landing attempt, providing a sense of engagement for all participants.

2.1 CONCEPT OF OPERATIONS

The VLR concept of operations is divided into five phases: (1) initialization; (2) ascent; (3) release and freefall; (4) controlled descent; and (5) landing. This is illustrated in Figure 2.

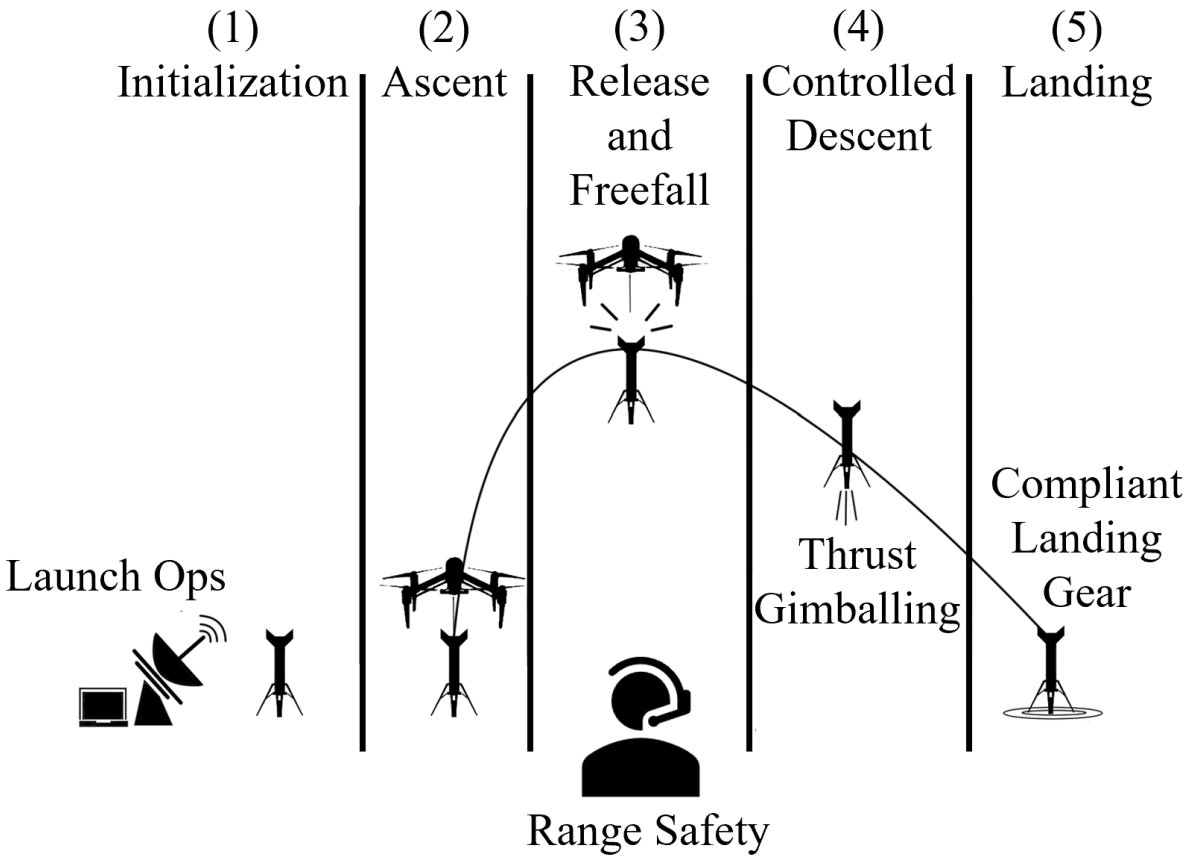

Figure 2: Concept of Operations Diagram

Initialization operations (1) requires a support personnel to connect the rocket motor igniter circuit to an ignitor inserted into the rocket motor, attachment of a disarming connector to the igniter circuit that opens the circuit from the battery to the ignitor, attaching the LiPo battery to the avionics battery input connector, attaching the drop tether to the UAV release mechanism, and finally powering the VLR for flight. A Roll Inhibitor separates the two lines of the drop tether to dampen the VLR's roll on take-off and ascent.

A checklist of all initialization and flight steps is followed by a Safety Protocol Officer at the launch site. This checklist consists of actions performed before and during flight as well as the list of all calls-outs made between the ground personnel. Once the VLR is powered on, the

Ground Station Operator connects to the VLR via SSH terminal protocol over a local Wi-Fi network, which is provided by a router on site, and the flight software routine is executed. The flight code checksum is confirmed to match the checksum shown on the checklist. The checksum serves the purpose of ensuring the correct version of the software is loaded and running. Once this is confirmed, another connection is made to the ground station via TCP/IP sockets. The day of launch barometric pressure is entered into the ground station prompt and uploaded to the flight software on the SSH terminal. The flight software collects sensor readings to calculate the gyro biases as the VLR rests in a static, upright position. The servos are then initialized, performing a range of movement test, going to five-degree extremes on both axes to ensure gimbal functionality. When ground personnel have observed this, the VLR is ready for lift off.

The ascent phase (2) consists of the takeoff by a UAV with the VLR suspended beneath it. During this time, the ground station shows the increasing altitude as determined from the onboard barometer. Once at the release height, the status of the ignition critical enable hardware is verified to ensure that the connector has not been accidently pulled during initialization or ascent. The UAV is stabilized and the VLR is ready for release from the UAV. A final software prearming command is sent to the flight software via SSH to enable an ignition signal prior to release. The release (3) from the UAV initiates a free-fall descent and disconnects the critical enable line from the top of the VLR. This allows current to be available for motor ignition.

Fins at the top of the VLR vertically stabilize it as its velocity increases in free-fall. Should the VLR exceed a 45-degree tip-over angle, the software is disarmed and the rocket motor inhibited from igniting. However, if the VLR is in a stable configuration, controlled descent operations (4) begin after motor ignition and the gimbal is used to maintain a vertical

orientation during the descent. The gimbal starts to move to positions commanded by the controller to correct for both rocket position and angular velocity errors.

Landing operations (5) begin once the rocket has touched down and consists of concluding data collection and powering down the system. Once the initial post-flight inspection is complete, VLR hardware is transferred from the landing zone back to the inspection tent. Hardware inspection and photo documentation, motor removal and disposal, and data collection and analysis all occur in this mode. The analysis reviews data from the ground station as well as the data stored onboard the VLR. Data sets are plotted to show the state of the VLR throughout the flight to the ground.

A group of designated launch personnel oversees all aspects of the concept of operations. The Range Safety Officer verifies launch conditions and monitors the range for any safety concerns. There are two Safety Personnel who are ready in case of a fire. One has a fire extinguisher and the other has a bucket of sand to dump on a fire if the extinguisher is unable to put it out. The Drone Operator is in charge of verifying the UAV's readiness for flight and all flight operations. The Ground Station Operator starts the flight software and connects to the VLR from the ground station. The Safety Protocol Officer ensures that the day of launch checklist is followed and adhered to. Additional Support Personnel are assigned as needed. Table 1 lists the personnel and their respective tasks.

Table 1: Designated Launch Personnel

Personnel	Number of Personnel	Responsibility
Range Safety Officer (RSO)	1	Has the overall responsibility for range safety. The RSO verifies clear sky and ground conditions prior to VLR launch and drop.
Safety Personnel (SP)	2	One SP is in charge of the fire extinguisher in case of a fire. One SP is in charge of the sand to dump on the VLR in case of a fire that is not extinguished by the fire extinguisher
Drone Operator (DO)	1	Is licensed to operate the UAV via remote control. has the responsibility of releasing the VLR.
Ground Station Operator (GSO)	1	Is responsible for calling out the progression of the software and enabling startup and drop.
Safety Protocol Officer (SPO)	1	Is responsible for managing day of launch checklist and protocols leading up to flight.
Additional Support Personnel (ASP)	as required	ASP are detailed as needed.

2.2 ROCKET DESIGN

The VLR fulfills the concept of operations by providing functionality with five physical subassemblies: the fin assembly; the avionics and avionics bay; the body tube; the gimbal assembly; and the landing leg assembly. Figure 3 shows the exploded VLR full assembly with the sub-assemblies grouped together.

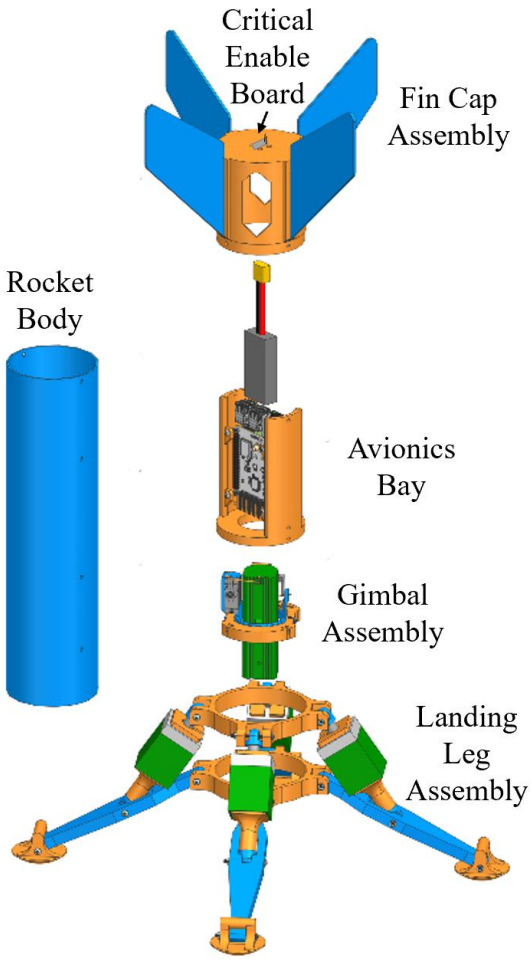

Figure 3: Exploded VLR Assembly

The table below summarizes the components of the physical system architecture that are described in detail in the sections that follow.

Table 2: Physical System Architecture

System	Component	Function	Interface
Structures	Body Tube	Main structure that houses the avionics, propulsive components, fins, and legs.	Fins Fin Cap Landing legs Aerodynamic fins Avionics Propulsion
	Landing Legs	Accepts the landing conditions and stabilizes the rocket upright on the ground.	Body tube
	Fins	Provides passive stabilization during the descent.	Body tube Fin Cap
	Fin Cap	Holds the four fins and connects to the rocket body. also acts as a connection to the UAV and holds the critical enable board.	Fins Critical Enable Body Tube
	Avionics Bay	Holds the Raspberry Pi and Navio2 in place in the center of the rocker.	Body Tube Raspberry Pi Navio2
Avionics	Raspberry Pi	Acts as the flight computer. Tracks the rocket progression as it steps through modes of flight. Reads in sensor values and computes gimbal control.	Navio2 Avionics Bay
	Navio2	Autopilot Hardware Attached on Top (HAT) for Raspberry Pi. Contains a dual inertial measurement unit (IMU), barometer, and GNSS receiver.	Raspberry Pi Avionics Bay X Axis Servo Motor Y Axis Servo Motor Ignition Board
	X Axis Servo Motor	Acquires position information from the Raspberry Pi, moving the gimbal as it receives the control response position	Navio2 Gimbal
	Z Axis Servo Motor	Acquires position information from the Raspberry Pi, moving the gimbal as it receives the control response position	Navio2 Gimbal
	Battery	Attached to the power module, which powers all of the components.	Power Module
	Power Module	Limits the voltage being sent to the Raspberry Pi and passes the power through to the ignition circuit as well as the Navio2 servo rail.	Battery Navio2 Ignition Board
	Two-Way Comms	Establishes communication with a ground station and transmits data during the flight. This also accepts information from the ground station and relays it to the flight software.	Raspberry Pi

Table 2 (cont.)

System	Component	Function	Interface
Avionics	Ignition Board	The ignition board relays the status of the critical enable to the Navio2 and sends a signal to ignite the motor when desired.	Navio2 Ignitor Critical Enable
	Critical Enable	Shorting pin that is pulled as the rocket is released, which is interrogated by the software to determine that the rocket has begun its descent.	Fin Cap Ignition Board
Propulsion	Motor	Provides a known impulse to slow the rocket as it descends.	Gimbal System Igniters Body Tube
	Igniters	Receives a current to heat up and ignite the propellant in the motor.	Motor Microcontroller
	Gimbal	Moved by the X and Y axis servos to maintain a vertical orientation during descent.	X Axis Servo Y Axis Servo Body Tube
Ground Station	Network Router	Provides a network for telemetry to be sent to the ground station and the VLR	Raspberry Pi Laptop
	Laptop	Hosts the ground station	Network Router

An avionics and software package provides the computational resources and sensor systems to determine the VLR's attitude, track the height above the ground, and enable the ignition system for the model rocket motor. The package also sends commands to the rocket motor steering gimbal to adjust its position to compensate for any VLR attitude and angular velocity errors. Power is supplied by a Lithium Polymer (LiPo) battery for the computer, sensors, ignition system, and gimbal servos. The VLR is also supported by a "ground system," which consists of a laptop computer capable of receiving wireless telemetry from the avionics package in proximity to a supplied wireless router. The physical system interfaces are provided in Figure 4.

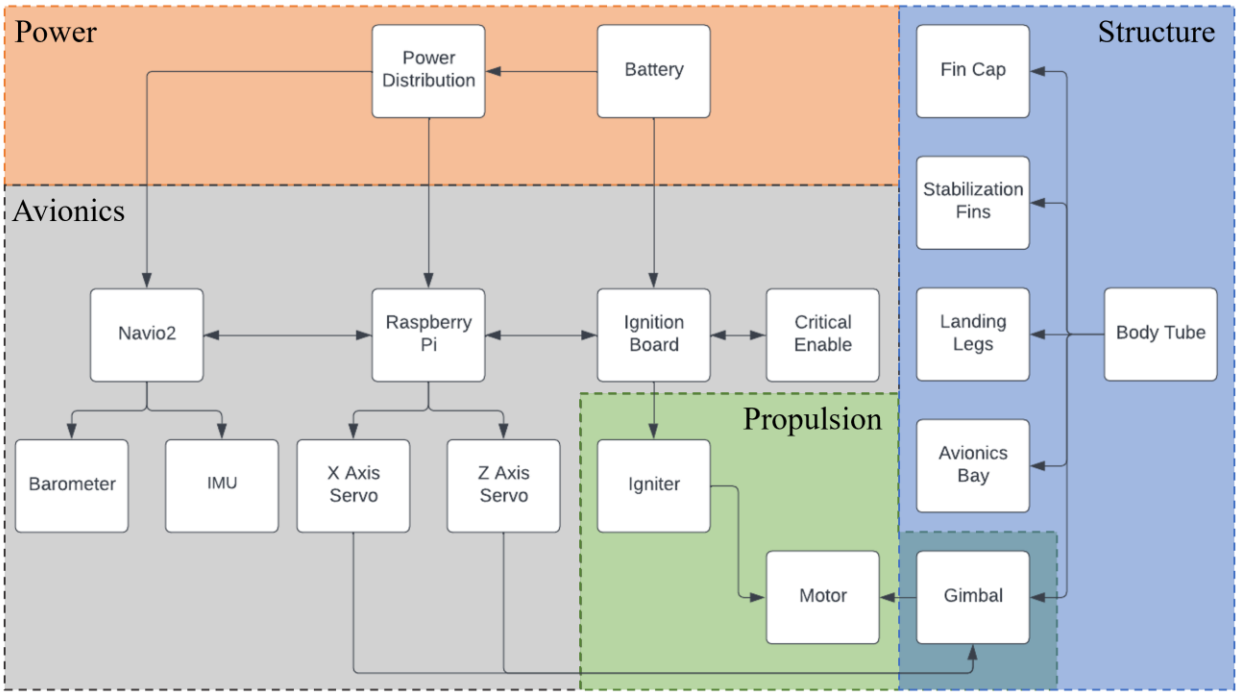

Figure 4: Interface Diagram

The VLR interfaces with the UAV through a rigging system that is used to connect the VLR to the UAV. This system is composed of three meters of fishing line wrapped around the UAV release pin, which is closed for take-off. The fishing line runs are held apart by a 3D printed Roll Inhibitor that discourages the lines from wrapping around each other on ascent. This system is shown in Figure 5**.** Once at release height, the UAV release system pin is pulled to drop the VLR. As the VLR falls away from the UAV, an ignition critical enable connector that is pulled from the VLR by fishing line that remains attached to the UAV. This ensures the motor does not ignite while attached to the UAV but starts the ignition timer when the VLR is released for descent and armed by a software command from the ground.

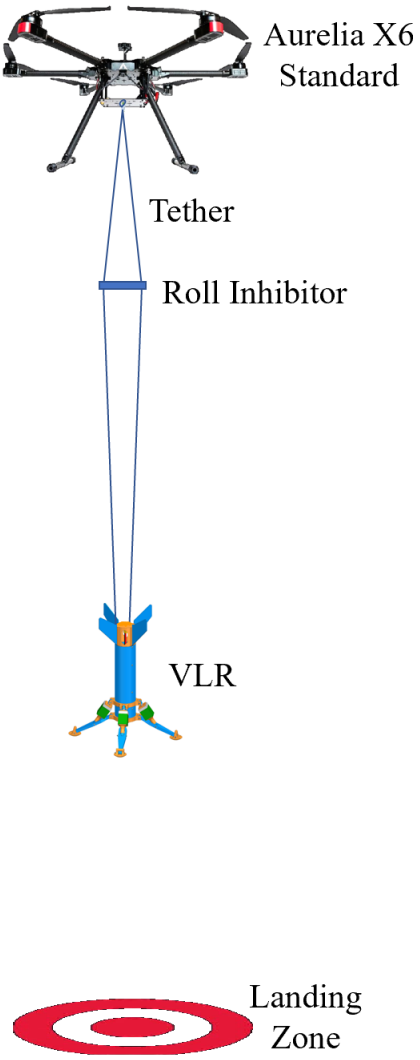

Figure 5: Interface between Aurelia X6 Standard and VLR

2.2.1 ROCKET BODY

The main structure of the rocket was initially made out of 75 millimeters of Blue Tube. This was selected as it is significantly stronger than a cardboard tube and not excessively heavy. The strength was believed to be worth the increased weight as it was intended to protect the avionics in case of a crash. However, after further analysis, it was determined that basic cardboard tubing is sufficient to protect avionics. As the strength is unnecessary, to conserve mass later evolutions of the design moved away from the Blue Tube. Looking at the original

design using Blue Tube (Figure 6), the rocket body is 14 inches long and has holes drilled in it to screw in and hold the internal components in place. This will be the same for the new design using the cardboard tubing.

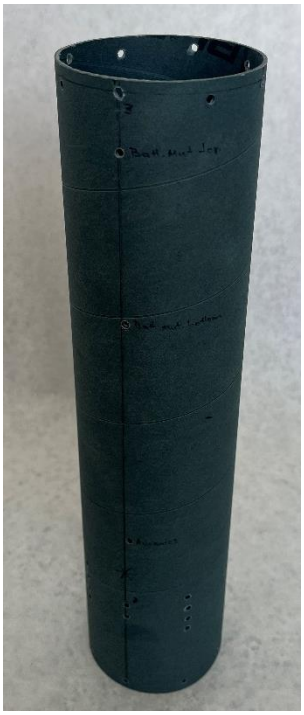

Figure 6: Rocket Body Structure

2.2.2 LANDING LEGS

The VLR has four landing legs that are symmetrically positioned around the base of the rocket and uses radio-controlled car shock absorbers as well as crushable foam structures to absorb the energy of landing. The legs and feet were designed in SolidWorks and then 3D printed using Polylactic Acid plastic (PLA) with an infill of 70%. The legs were initially printed with a lower infill but failed in preliminary drop tests. While selecting the infill percentage, it is important to note that increasing the infill percentage beyond 70% has diminishing returns of strength and requires more material and longer print times. The legs were designed to be geometrically simple and easily printed with minimal support structure.

From initial drop testing, it was determined that the legs would need a way to absorb energy at touchdown to prevent the VLR from bouncing or legs from breaking, so a design with sprung shock absorbers from a model car was developed. However, the shock absorbers did not sufficiently dissipate landing energy, resulting in broken landing legs or tip-overs. Another means of dissipating the energy of landing was required.

A suitable solution was formulated from green floral foam and white Styrofoam wrapped around the supporting shock absorber structure. Plungers on either side of the foam sandwich crushes the foam and absorbs most of the energy in the process. The legs attach to the VLR with a top and bottom ring that are screwed onto the body tube. Figure 7 shows the final landing leg assembly.

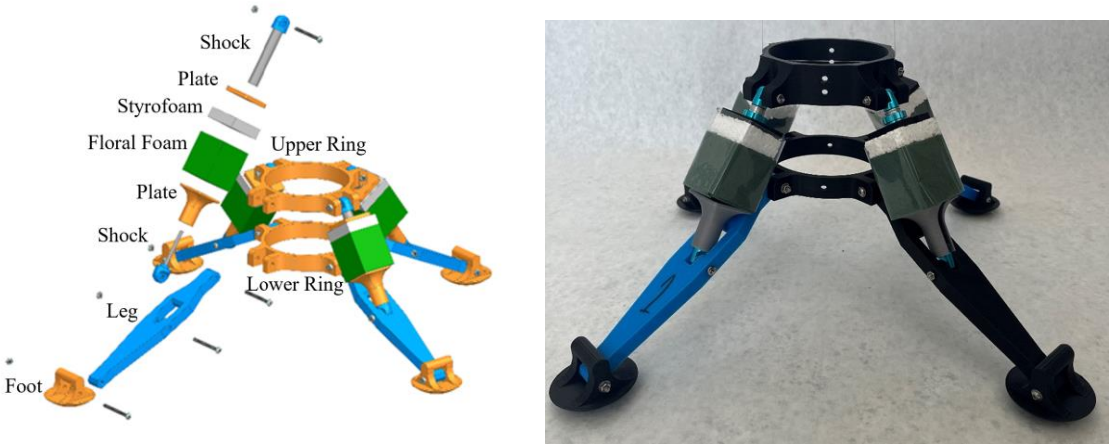

Figure 7: Landing Leg Assembly

The feet are rounded attachments that connect to the ends of the legs. They are designed to have a rounded bottom to allow them to brush over uneven surfaces and not catch on objects on the ground. The feet are capably of pivoting 20 degrees in both directions on one axis. To limit the rotation, a bar is above the attachment point to the legs. Figure 8 shows one of the feet with the attachment to the leg and the movement inhibiting bar above said attachment. Further

design justification and analysis can be seen in “Design Development of a Vertically Landed Model Rocket” by David Gable.

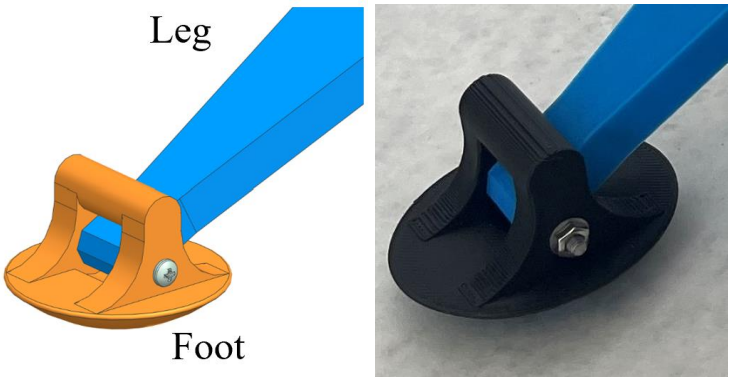

Figure 8: Landing Leg Foot

2.2.3 AERODYNAMIC FINS

Aerodynamic fins are located on the top of the rocket. The design is shown in Figure 9. The fins are slotted into a 3D printed end cap covering the avionics bay and were designed to be held in place by the rocket tube itself acting as a lower stop. Due to printer error and tolerances, the fins were often either too wide and could not be slid into the fin cap or were too thin and were able to move around in the installation. This led to the decision to print them marginally smaller and epoxy the fins into the fin cap. The shape of the fins was dependent on the fins being printed using PLA while still being able to provide stability. If the fins were too thick, the time the layer took to print meant that the PLA would start cooling before the next layer was added on top, causing the print to crack and warp, however if they were too thin, they would not be sufficient to stabilize the rocket. To find the optimal size of the fins, a thin airfoil theory analysis was performed. This process was undertaken by using the area of two fins and solving for the lateral force that can correct to a straight orientation. Repeating this with varying angles and solving for the lift force allowed for the lateral force to be found. Using this analysis, the fin size

was determined. Looking at the fin cap, the holes on the side were designed to save mass and to make the rocket body inside more accessible. This allowed for an easier assembly when attaching the fin cap as well as plugging in the battery to power the system.

The fin cap is also the attachment point for the VLR lifting tether to the UAV. The current design has a tube that allows the harness to be threaded through and attached to the UAV. The top of the fin cap has the critical enable pins mounted so that a tethered connector can also be attached to the UAV. Figure 9 on the left shows the fin cap assembly with the tube for the harness attachment and the exploded assembly.

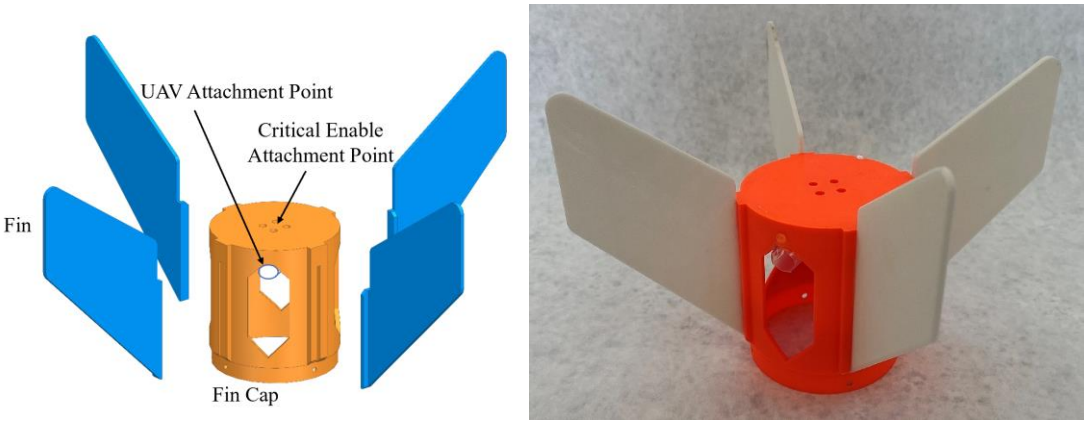

Figure 9: Fin Cap Assembly

2.2.4 AVIONICS BAY

The avionics bay was designed to hold a Raspberry Pi processor and Navio2 controller in place with space for the wiring and other components to fit alongside it in the main tube. The avionics bay is shown in Figure 10. The Raspberry Pi and Navio2 are held in the avionics bay by screws in the four corners on both sides. The avionics bay was designed to be easily printable, starting on the base and printing up to the top. The battery is mounted above the avionics on the inside of the rocket body and velcroed onto the wall. Looking at the bottom of the avionics bay,

there is a circular pass through for wires to the gimbal system and ignitor. This is located below the servo rail on the Navio2 so that the gimbal servo wires can pass through. This also allows for the ignition line's alligator clips to be passed through to the ignitor inserted in the rocket motor.

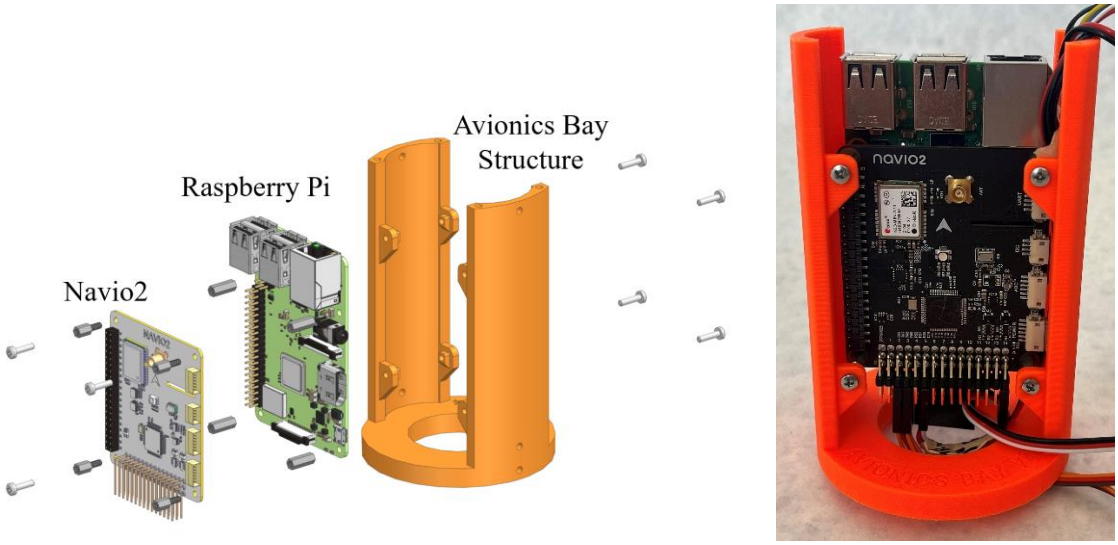

Figure 10: Avionics Bay

2.2.5 DECELERATION SYSTEM

The gimbal has two degrees of rotation, moving in the X and Z axes with five-degrees maximum excursion in each axis. The gimbal is placed inside the rocket body and screwed into place near the bottom of the tube. A hollow plastic tube inside the gimbal assembly holds the model rocket motor used to decelerate the vehicle for landing. As the gimbal is set inside the body tube, the servo arms were designed to fit within the inner diameter and allow for their rotation as they steer the motor. The inner gimbal ring is 3D printed in two separate parts epoxied together to attach the arm that holds the servo to the inner ring. Figure 11 shows the gimbal design and assembly.

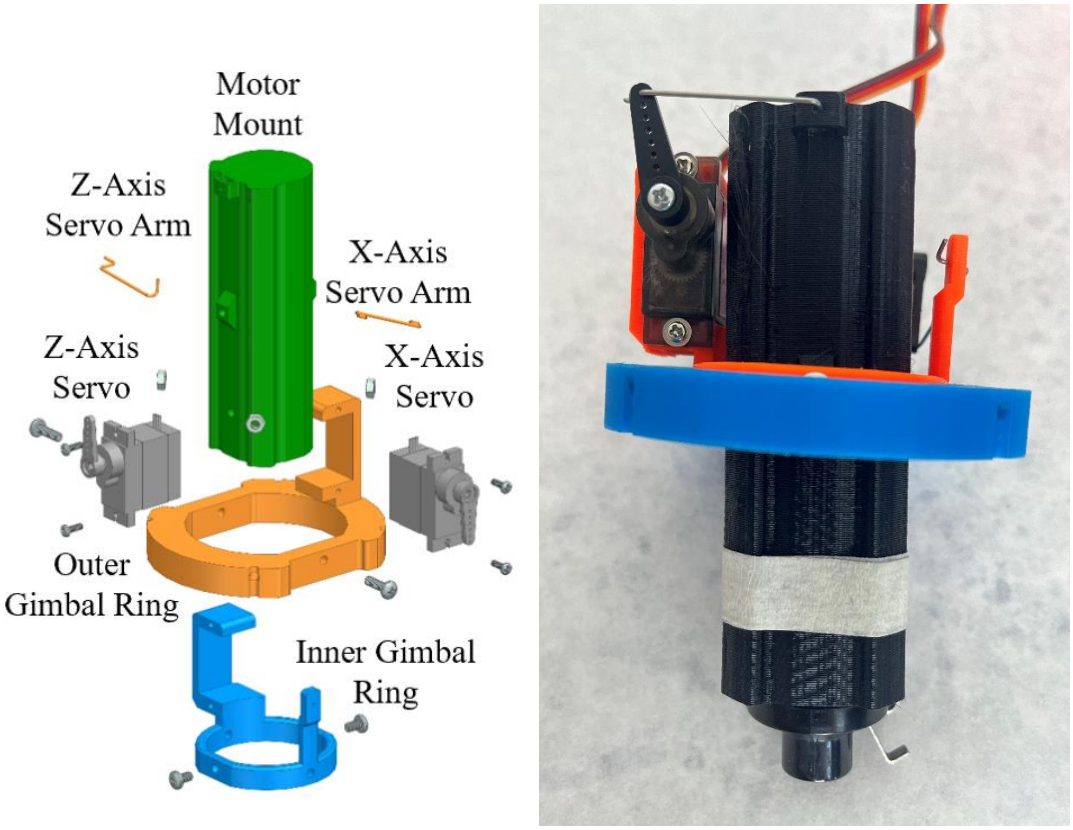

Figure 11: Gimbal Assembly

2.2.6 SOLID ROCKET MOTOR

A MATLAB simulation was used to establish VLR performance parameters used in sizing the rocket motor, height of release, and ignition delay time. Based on these simulations, an Aerotech E20W-7 motor was initially selected to decelerate the VLR for landing. This motor was selected due to its average thrust output of 22.2 N and a burn duration of 1.6 seconds. Figure 12 illustrates the thrust curve for the motor as provided by ThrustCurve.org [9]. The motor performance was tested and verified through a series of thrust tests discussed in Chapter 3.

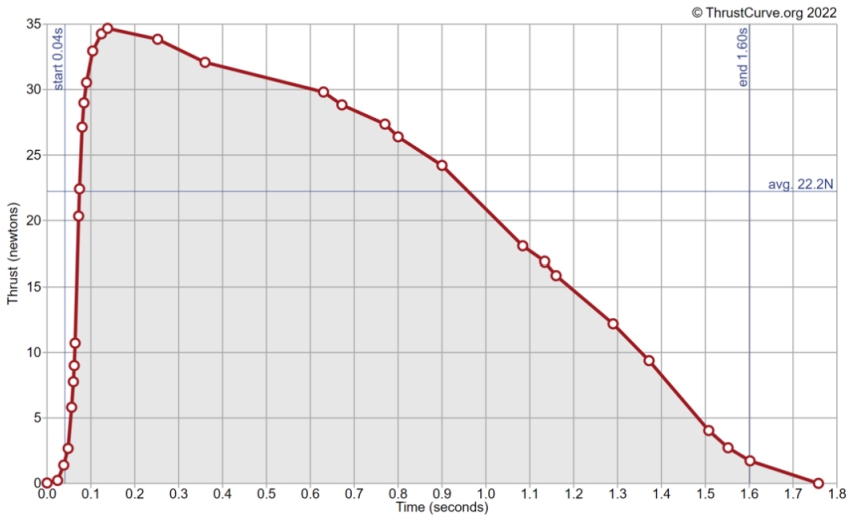

Figure 12: Aerotech E20W-7 Thrust Curve

2.3 AVIONICS

2.3.1 ONBOARD COMPUTER

The VLR's onboard computer is a Raspberry Pi 3 B+. The Raspberry Pi 3 B+ is a quad-core 64-bit 1.4 GHz computer, with 1GB of RAM, and uses a 32 GB microSD card for telemetry data storage [10]. A Navio2 Autopilot HAT interfaces with the Raspberry Pi to provide attitude data and control the gimbal servos [11]. The Raspberry PI 3B+ and Navio2 assembly is shown in Figure 13.

Figure 13: Raspberry Pi 3B+ and Navio2 Assembly

2.3.2 INERTIAL MEASUREMENT UNIT

The Navio2 IMU is a nine degree of freedom system incorporating a MPU9250 and a LSM9DS1 to sense rates, accelerations, and magnetic fields. For this project, the MPU9250 was prioritized for its wider full-scale ranges. The accelerometer has a full-scale range of ±16g, the magnetometer has a full-scale range of ±4800μT, and the gyroscope has a full-scale range of ±2000°/sec [12].

2.3.3 BAROMETER

The Navio2 contains a MS5611 component, which is a high-resolution barometer. This barometer has a pressure range of 10 mbar to 1200 mbar and a temperature range of -40°C to 85°C. The sensor resolution is 10 cm for the altitude, 0.012 mbar for the pressure, and 0.01°C for

the temperature [13]. Using the pressure and temperature data, the altitude of the VLR is monitored throughout the flight.

2.3.4 POWER

A 650 mAh LiPo battery powers the avionics. This battery satisfies the system power budget, later shown in Table 8, assuming all capabilities aside from ignition are used for 15 minutes. The battery is attached to a power module that distributes power to the system through the Navio2. Also attached to the battery is a battery elimination circuit (BEC) that is tied to the servo rail on the Navio2. The ignitor is attached to a stand-alone ignition board and a critical enable board (both designed in-house) that receive power from the battery and a signal from the Raspberry Pi. Figure 14 shows the VLR's power circuit.

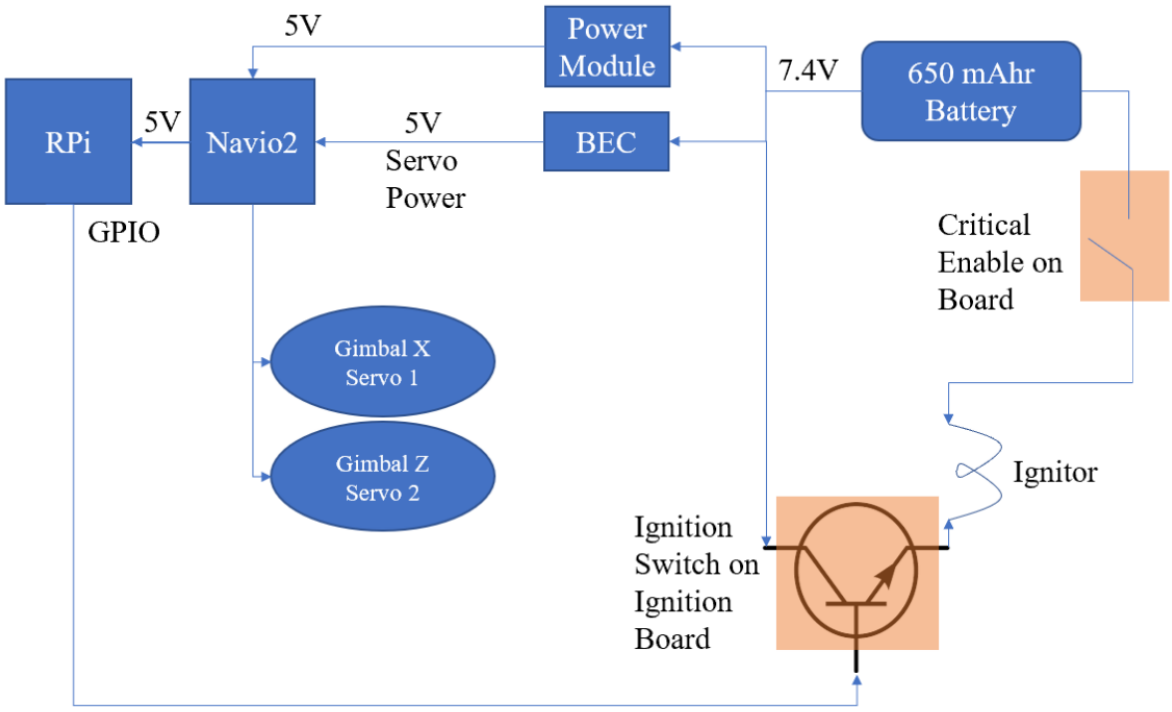

Figure 14: Power Circuit

The ignition board and the critical enable circuit schematics are shown in Figure 15 and Figure 16 and provide two factors of safety. If the ignition board receives a signal to ignite and the critical enable connector has not been pulled, there will be no ignition. In the same way, if the critical enable is pulled but the ignition board has not received an arming signal from the flight software to ignite, there will be no ignition.

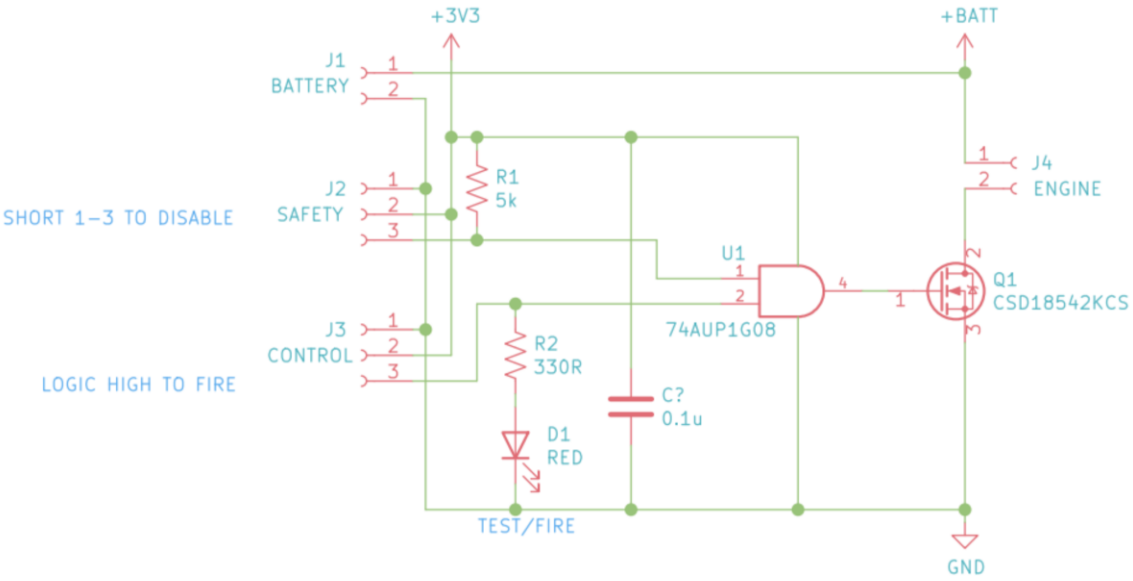

Figure 15: Ignition Board Schematic

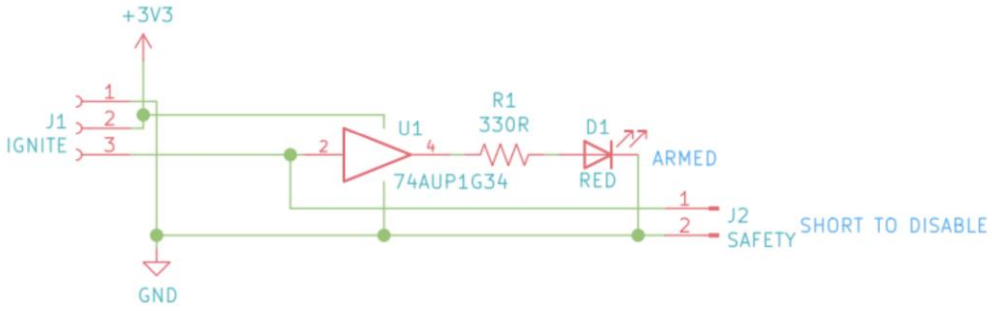

Figure 16: Critical Enable Board Schematic

2.3.5 GROUND STATION

A wireless laptop serves as a ground station (GS) connected to the VLR via TCP/IP through a local wireless router. The VLR receives initialization confirmations and inputs for the day of launch barometric pressure from the ground station. The data transfer interface provides a visualization of VLR attitude and a backup of the flight telemetry data. The GS receives attitude data, IMU data, power levels, critical enable status, time, mode, height, and servo control responses.

The display in Figure 17 shows received data plots as well as general status information. Note that this figure was a ground station test plot and had altered required mode changes to see the progression without needing to lift and release the rocket. At the top of the display the mode, time of flight, battery voltage, ignition timer, height, and critical enable status are displayed. This allows the Ground Station Operator to monitor the flight to verify the progression of the modes, and to ensure that the critical enable has not been pulled prior to release. This data allows for a safe abort should an abnormal or unsafe condition be indicated.

The top left of the display shows a box that represents the orientation of the VLR. This allows the Ground Station Operator to ensure that the attitude control of the rocket is acting nominally and tracking the attitude correctly. The x-axis of each plot is the most recent 100 data points received.

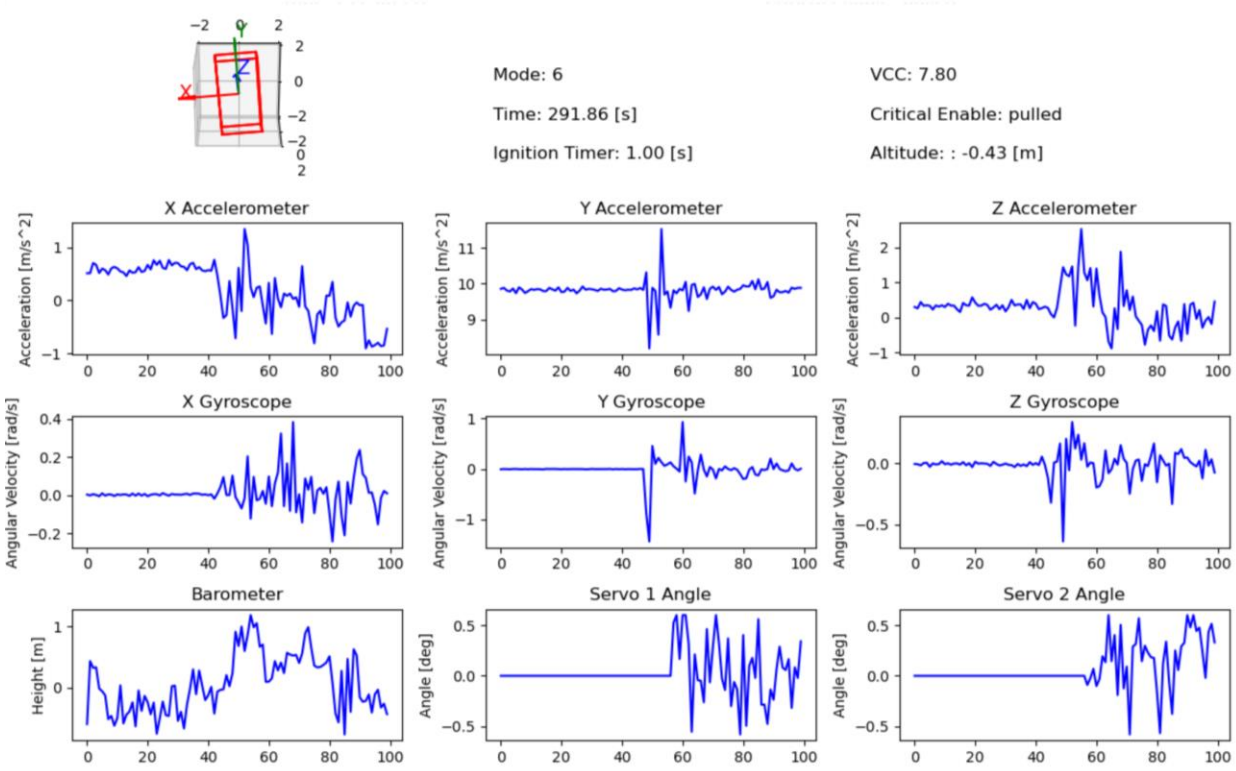

Figure 17: Ground Station Display

2.4 UNMANNED AERIAL VEHICLE

The UAV utilized for this project is an Aurelia X6 Standard, shown in Figure 18. This UAV was selected due to its ability to carry loads up to 5 kg. This UAV also has a large payload bay that allows for the release mechanism attachment. The Aurelia X6 Standard utilizes an open-source Pixhawk flight controller and is set up with Ardupilot software. This UAV has a maximum flight time of 30 minutes and a maximum station keeping wind resistance of 20 mph [14]. With the knowledge that the UAV carries the VLR hanging from a tether, subjecting the flight system to additional variable loads from the underslung payload, the VLR was designed to weigh less than 1.5 kg.

Figure 18: Aurelia X6 Standard

2.5 PERFORMANCE BUDGETS

2.5.1 MASS BUDGET

The mass of the VLR is broken down into subassemblies. The gimbal assembly includes the gimbal structure, servos, and the motor that it holds. The avionics bay assembly includes the structure that holds all the avionics. This includes the Raspberry Pi, Navio2, ignition circuit and power system. The structures subassembly includes the main body as well as the fin cap assembly. The landing leg assembly includes the printed legs, rings, shocks, foam, and feet. These subassembly masses are shown in Table 3-Table 6.

The mass of each subassembly and their respective percentage of total mass are shown in Table 7. This table also shows that the rocket was below the mass requirement of 1.5 kg.

Table 3: Gimbal Mass Budget

Component	Material	Quantity	Mass [g]
Gimbal Tube	PLA	1	22.89
Gimbal Inner Ring	PLA	1	6.17
Gimbal Outer Structure	PLA	1	17.17
MG90S and Steel Wire	N/A	2	28.17
Screw M3 5mm	Steel	4	2.44
Screw M2 6mm	Steel	4	0.91
Rocket Motor	N/A	1	9.7
Total			87.45

Table 4: Avionics Bay Mass Budget

Component	Material	Quantity	Mass [g]
Avionics Bay	PLA	1	41.19
Raspberry Pi	N/A	1	45.00
Navio2	N/A	1	23.00
LiPo Battery	N/A	1	43.00
Power Module	N/A	1	17.00
BEC	N/A	1	9.00
Panhead Screw M2.5 10mm and Nut	Steel	8	5.88
Panhead Screw M3 10mm	Steel	4	3.25
Ignitor Circuit	PCB	1	5.39
Total			192.71

Table 5: Structures Mass Budget

Component	Material	Quantity	Mass [g]
Rocket Body Tube (~14"/355 mm)	High Density & Strength Paper	1	166.25
Fin Cap	PLA	1	55.08
Fin	PLA	4	48.04
Glue	Adhesive glue	1	25
Total			294.37

Table 6: Landing Legs Mass Budget

Component	Material	Quantity	Mass [g]
Lower Ring	PLA	1	54.00
Upper Ring	PLA	1	39.00
Landing Legs	PLA	4	58.40
Landing Feet	PLA	4	30.80
Screws	Steel	16	26.56
Hex Nuts	Steel	16	5.44
Washers	Steel	32	4.48
Shock Absorbers	Aluminum/Steel	4	113.68
Crushable Structure	Foam	1	30.00
Total			362.36

Table 7: Total Mass Budget

Assembly	Total Mass [g]	% of Total Mass
Gimbal	87.45	9.06
Avionics Bay	192.71	19.96
Structure and Aerodynamics	294.37	30.49
Landing Legs	362.36	37.53
Cabling/Harnesses	28.69	2.97
Total	965.58	100

2.5.1.1 CENTER OF GRAVITY AND CENTER OF PRESSURE

The center of gravity of the VLR is centered horizontally and within the rocket at 142 millimeters high from the bottom of the body tube. Figure 19 shows this location.

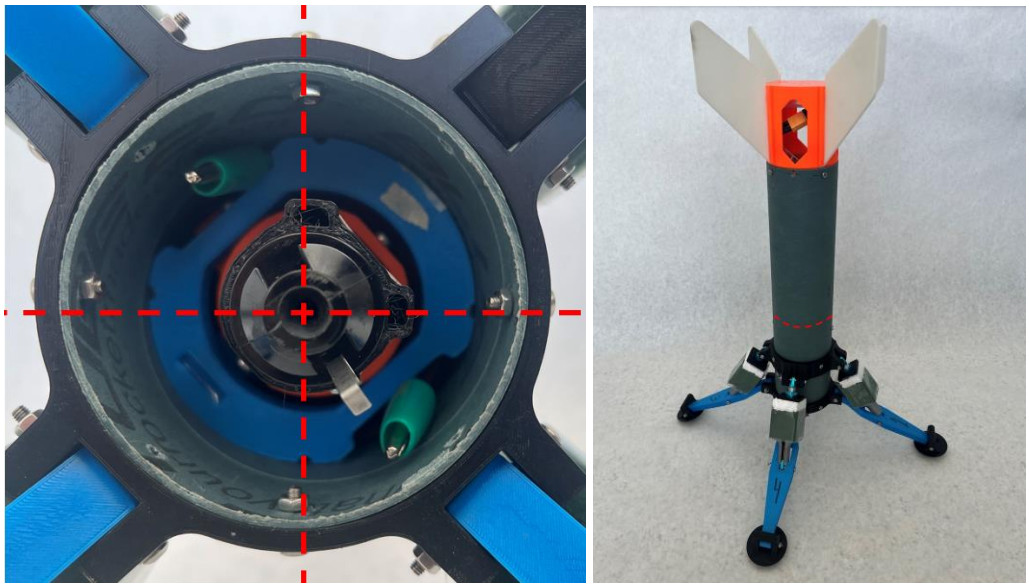

Figure 19: Center of Gravity Location

Finding the center of gravity location can be done by suspending the VLR from a string that is moved along its long axis until the rocket balances. This method is demonstrated in Figure 20.

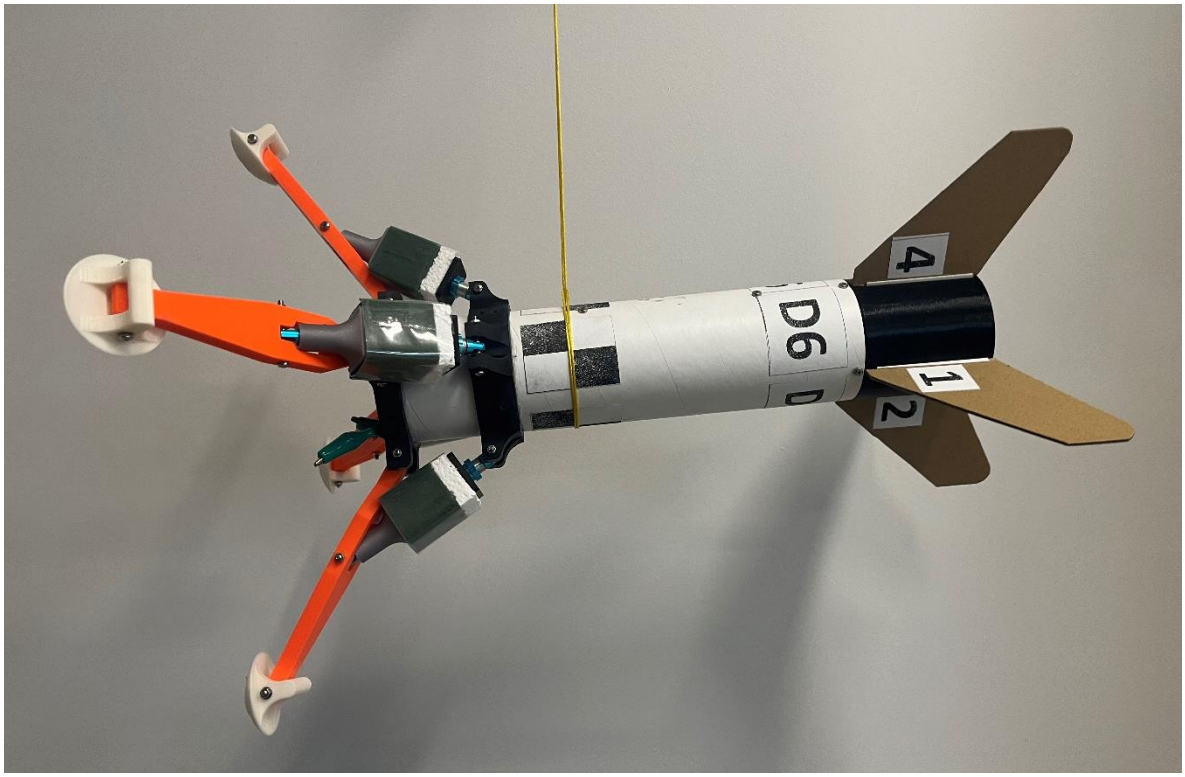

Figure 20: Center of Gravity Determination

To have a stable rocket, the center of gravity needs to be below the center of aerodynamic pressure. The team accomplished this by essentially designing the fins in a way that they were large enough to ensure that the center of pressure had to be above the center of gravity. This stability was tested and validated in the series of drop and wind tunnel tests.

2.5.2 POWER BUDGET

The power budget, provided in Table 8, was analyzed assuming a requirement for 15 minutes of powered avionics operations. Power consumption of most components of the VLR system vary depending on what mode of flight the rocket is in; however, this power budget was created assuming all components were consuming maximum power for the duration of the powered vehicle time aside from the ignition circuit. Looking at the total system energy of 1.92 Whr, it can be seen that the battery selected is more than sufficient as it can provide 4.81 Whr. In

addition, this power usage will result in a depth of discharge around 39.1%, which is ideal as having a smaller depth of discharge extends useful LiPo battery life

Table 8: Power Budget

Component	Quantity	Voltage [V]	Current [mA]	Efficiency [%]	Power [W]
Raspberry Pi	1	5	500	90	2.78
Navio2	1	5	150	90	1.67
MG90S	2	5	100	80	3.13
*Ignitor Circuit	1	7.4	12650	100	93.61

Total Power Normal Operations	7.58 W
Total Power During Ignition	101.19 W
System Energy	1.92 Whr
Battery Energy	4.81 Whr

* denotes on for 1 second

2.6 FLIGHT SOFTWARE DESIGN

The flight software is designed to operate autonomously after receiving day of flight information and a software arming command from the ground station via SSH terminal inputs from the operator. The software then launches seven additional threads that manage the VLR throughout its flight. The threads manage telemetry, data storage, gimbal control, attitude tracking, voltage and height monitoring, critical enable status, and prints for debugging. After launching each thread, the software moves into a while loop that tracks the progress of the flight as it steps through the various modes. The software remains in the while loop until landing, at which point it joins all the threads and terminates them after saving the flight data.

2.6.1 OPERATIONAL SOFTWARE MODES

The flight software is written in C++ and steps through a switch/case construct that determines what point of the flight the VLR is in, performing appropriates tasks for each mode.

A description of each software mode follows the modes and states diagram that is provided in Figure 21.

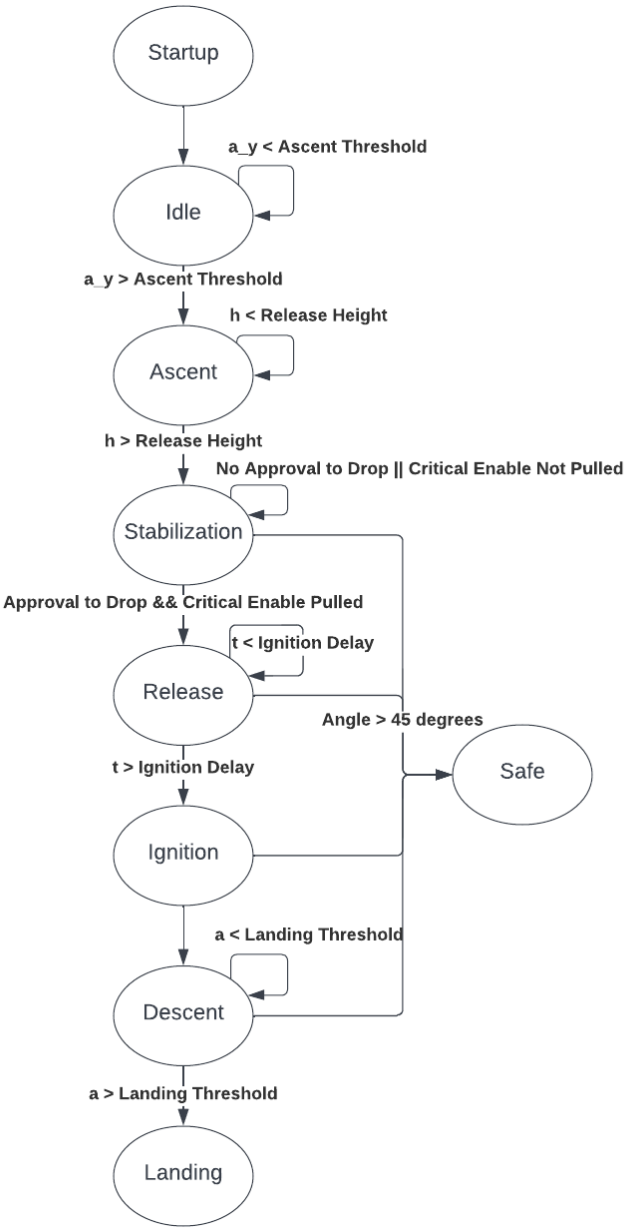

Figure 21: Operational Mode Progression

2.6.1.1 STARTUP

Startup mode begins with connecting the ground station and conducting a test of the gimbal, moving through the 5-degree range control on both axes. Once the gimbal test has been completed, the next mode is entered.

2.6.1.2 IDLE

Idle mode is transitioned into once the startup has been completed and the VLR is awaiting ascent. The VLR remains in this mode until the accelerometer indicates the VLR has been picked up by the UAV.

2.6.1.3 ASCENT

Ascent mode transition occurs after the VLR is lifted by the UAV and begins moving upwards. The VLR remains in this mode until the release height is reached. To combat barometric noise, the release height is first exceeded by the UAV in order to trigger the mode change and then the UAV is commanded to descend to the release height. Once this release height is reached, transition to stabilization mode occurs.

2.6.1.4 STABILIZATION

Stabilization mode begins with the VLR reaching the desired release height. The VLR sends a message to the terminal asking, “Proceed with drop?” The mode progression looks for this approval to arm as well as the physical critical enable signal. Opening the critical enable pin located at the top of the VLR sends a signal to the software indicating descent has begun. Both conditions must be met for the VLR flight software to progress to the release mode. During the flight, the ground station operator will check with the Drone Operator to see if are ready to drop. Once this confirmation is received, the ground station operator will give the drop confirmation

command and notify the Drone Operator. The Drone Operator then notifies all personnel that he/she is dropping the VLR, the UAV releases the VLR, and the critical enable pin is pulled off the top of the VLR as it falls. The VLR then enters release mode.

2.6.1.5 RELEASE

As Release mode is entered, a timer starts immediately and counts down until ignition. Once this timer expires, the VLR progresses to the ignition mode.

2.6.1.6 IGNITION

Ignition mode is entered once the ignition delay timer expires. This mode sends a signal to the ignition board to ignite the motor. Once the signal is sent, the rocket transitions into the descent mode.

2.6.1.7 DESCENT

Descent mode is entered after ignition of the motor. The gimbal control is determined using a proportional derivative (PD) controller that monitors VLR orientation and rotational velocity to determine the reaction needed from the gimbal. The VLR remains in this mode until the sensors indicates that the rocket has landed.

2.6.1.8 LANDING

Landing mode is entered as the sensor readings show the rocket is no longer descending. This mode terminates all the threads and ceases all communications. This mode also ends data collection and closes the data files. Once this has been accomplished, the software terminates execution.

2.6.1.9 SAFE

Safe mode can be entered once the rocket is at the release height. This mode is entered when the rocket is tipped more than 45-degrees from the vertical orientation. This is due to the rocket being unable to recover to a vertical orientation if this offset has been reached. The safe mode halts all flight progression and sets the gimbal to be straight down and sends no signal to ignite.

2.6.2 FLIGHT SOFTWARE ARCHITECTURE

The flight software is organized into one main function and seven threads allowing for multiple tasks to be performed simultaneously.

2.6.2.1 MAIN FUNCTION

The main function is where all the threads are launched. After launching the threads, this function moves to a while loop that evaluates the state of the VLR until it lands. This while loop is where the mode transitions are commanded. Once the VLR lands and the loop is exited, all threads terminate.

2.6.2.2 TELEMETRY THREAD

The telemetry thread stores orientation, sensor, time, power, and control data on the Raspberry Pi for later analysis. The thread obtains and stores data found in other threads and saves it into a CSV file.

2.6.2.3 GROUND STATION THREAD

The ground station thread establishes the connection between the VLR software and the ground station and sends data between the two. This thread sends flight critical data to the ground station so that the progress of the VLR can be manually checked. The ground station is

set up to show the sensor readings as time progresses, as well as the mode, time, and critical enable status.

2.6.2.4 ATTITUDE DETERMINATION THREAD

The attitude determination thread tracks the orientation of the rocket. This is done utilizing the IMU readings for the acceleration, rotation, and magnetic field that the VLR is experiencing. A Madgwick filter is utilized to correct for noise in the sensor readings. The Madgwick filter is an orientation filter for IMUs with tri-axial gyroscopes, accelerometers, and magnetometers [15]. This filter functions by representing the VLR orientation in quaternions, allowing the accelerometer and magnetometer data to be used in an optimized gradient descent algorithm to find the gyroscope measurement error as a quaternion derivative [16].

To implement this filter, the gyroscope and accelerometer biases must be determined. To find the magnetometer biases, the avionics are placed in a known orientation, and the magnetometer readings are saved. The orientation is then flipped in all three axes and the same magnetic field is measured. If the sensor does not provide the same reading with opposite sign in each direction, then the difference represents the bias in the sensor. This bias is then provided to the filter. This filter allows for a much more accurate and robust attitude estimation.

2.6.2.5 GIMBAL CONTROL THREAD

The gimbal control thread is launched after initialization is completed, but this thread is not actively computing the control response until the rocket is released from the UAV. The control response is found using a PD controller. This controller uses the orientation and the angular rates to calculate the torque required to upright the VLR about the X and Z axes. Below shows the equations used to find the ideal torque.

$$\tau_x = K_p * q_1 - K_d * g_x \quad (1)$$

$$\tau_z = K_p * q_3 - K_d * g_z \quad (2)$$

where

q_1 = scalar x component of orientation quaternion

q_3 = scalar x component of orientation quaternion

g_x = x gyroscope reading [deg/s]

g_z = z gyroscope reading [deg/s]

K_p = position gain

K_d = rate gain

For this control law implementation, the response of the system in the X axis only is demonstrated in Figure 22. This system defined gains of $K_p = 0.075$ and $K_d = 0.02$. Looking at the angle from vertical, it can be seen that the system is stable and capable of converging to zero.

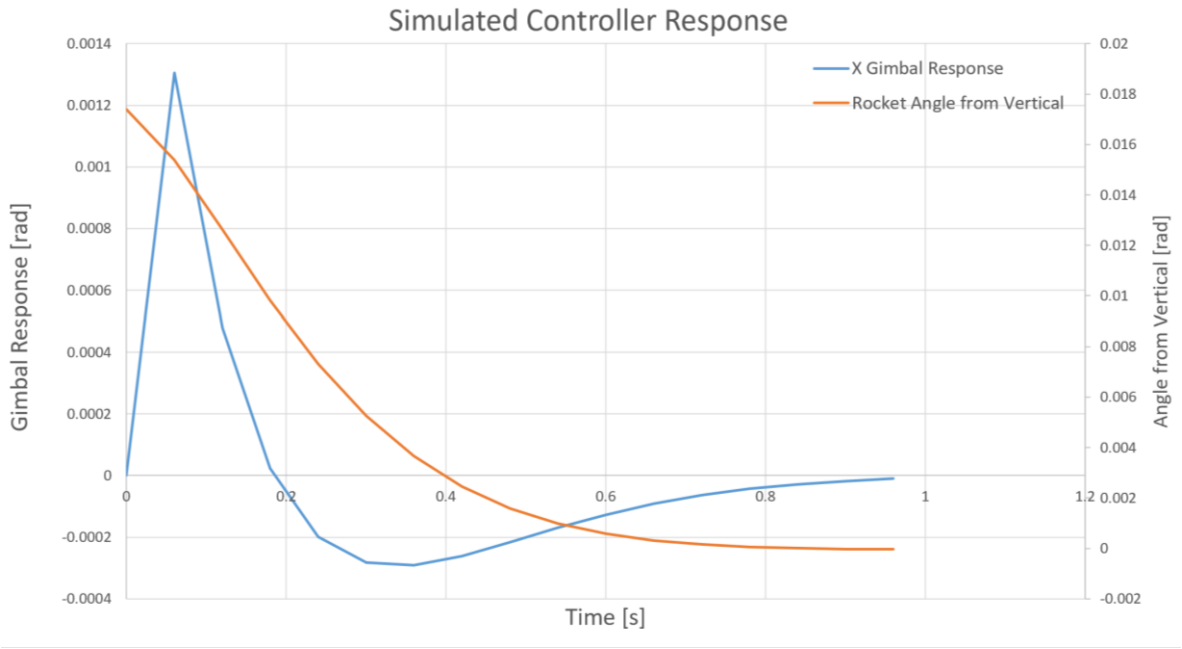

Figure 22: Simulated Control Response in One Axis

From the found torque, the forces, F_x and F_z, needed about the axes can be found.

$$F_x = \frac{\tau_z}{L} \tag{3}$$

$$F_z = -\frac{\tau_x}{L} \tag{4}$$

where

L = length of gimbal lever arm [m]

This force is then used to find the angle of the gimbal, with the gimbal angle being limited to a maximum of five degrees. If the found angle is over five degrees in any direction, the gimbal is set to ±5 deg.

$$\varphi = \sin^{-1}\frac{-F_x}{T} \tag{5}$$

$$\theta = \sin^{-1}\frac{F_Z}{T} \tag{6}$$

where

T = Motor Thrust [N]

This thread continues computing the control response until landing or safe mode has been reached.

2.6.2.6 HEIGHT AND VOLTAGE THREAD

This thread serves two purposes, it tracks the height of the VLR, and it tracks voltages of various channels. This thread supports two functions as neither are time critical, so they can be grouped together as additional data collected. The height of the VLR is used only as a flag to ensure the motor cannot be ignited on the ground. The height is found using the base altitude found from the day of launch conditions and height of the rocket at initialization and subtracting that from the current altitude which is found using data from the barometer. The voltage data is for later analysis on power consumption as well as ensuring the battery has sufficient charge for the flight. The ADC continuously measures voltage on all six channels available on the Navio2. The channels are as follows: board voltage, servo rail voltage, voltage and current on the power module, and two channels in the ADC connector.

2.6.2.7 DROP ENABLE THREAD

The drop enable thread is not executed until the stabilization mode has been reached. Once that mode has been reached, it requests approval to drop. Once received, this thread sets flags depending on what response was taken. This thread has no further function after an answer has been provided.

2.6.2.8 PRINT DEBUG THREAD

This thread prints out various states and variables for purpose of debugging. This prints to the terminal, which can cause the software to run slower than optimal. For this reason, this thread is not launched in the flight ready software but can be uncommented to launch when debugging.

CHAPTER 3: VERIFICATION, SIMULATION, AND TESTING

3.1 THRUST STAND TEST

The test stand utilizes an Adafruit load cell, an amplifier, and a Teensy 4.0 microcontroller to measure the thrust force produced by the motor. Test stand operation and safety documentation were established and followed for all motor tests.

The thrust stand is created out of T-slotted aluminum manufactured by 80/20 [17]. These components are easy to work with and are adaptable for changes in the stand design. The motor mount is made of a 3D printed PLA tube within which the motor sits. The original test stand had the motor horizontally positioned but was later changed to be vertical to mitigate a possible horizontal ejection of the motor in a failure.

To characterize the motor, the test stand has a load cell. The load cell utilizes a strain gauge to measure force applied with a HX711 Amplifier. The load cell used on this test stand is a 20 kg load cell. A set of brackets were used to mount the load cell to the thrust stand structure. These were custom designed and manufactured out of aluminum.

To read the data from the HX711 Amplifier, a Teensy 4.0 Arduino-based microcontroller was utilized. For the recording program, an HX711 Amplifier library was used [18]. The recording program marks time of ignition as indicated by the ignition circuit, then stores data points and the time each data point was taken in an array, and outputs the results through the serial port. A piece of freeware called CoolTerm [19] was used to record the data. Figure 23 shows the thrust test stand with a motor mounted vertically in it.

Figure 23: Thrust Stand

The ignition circuit used is the same as the one used on the VLR. When a signal is sent to the ignition circuit, in this case, by flipping a switch, the ignition circuit ignites the motor and signals to the Teensy 4.0 that it has ignited the motor. A battery is connected to the ignition circuit to provide enough energy to ignite the rocket motor.

Figure 24 shows five thrust tests using the Aerotech E20W-7 [9] motor stacked on top of each other. There were six tests conducted, however, the fourth test did not ignite, thus there is no thrust curve present on the plot. The expected thrust curve is also provided for reference. One significant variable that needed to be characterized was the ignition delay, which with this motor varied by nearly 0.5 seconds. As four of the five successful tests had similar delay times, it is likely that the ignitor was improperly inserted into the motor for the sixth test. Looking at the other four data sets, they all seem to reach the desired magnitude of thrust, albeit slightly slower than the expected thrust curve. Feeding the thrust curves back into the MATLAB simulation showed that the real performance of the motor was feasible for landing the VLR and allowed for more confidence in selecting launch parameters.

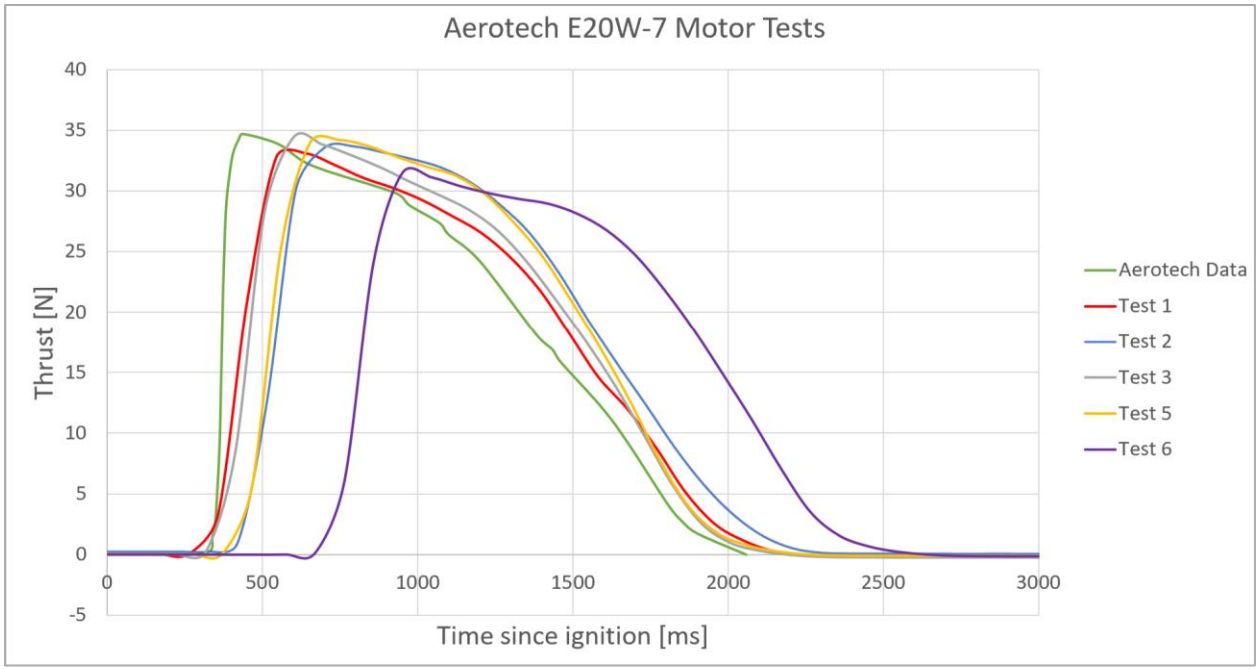

Figure 24: Aerotech E20W-7 Thrust Curves

This testing was critical to simulating the behavior of the rocket during descent and its value was proven when several instances of rocket motors not replicating their published thrust curves were observed in testing. The Aerotech E11J-3 did not follow its published curve, underperforming significantly. After conducting numerous tests and recalibrating the load cell, the manufacturer was contacted and, after conducting tests of their own, acknowledged that propellant formulation changes were not followed up with changes to the published performance specifications.

3.2 MOTOR/GIMBAL TESTING

To verify the ignition circuit as well as the software's ability to ignite, gimbal, and retain connection with the ground station during operations, an ignition test was conducted. This was done on a custom-made test stand that would allow for the ignition and one degree of freedom for moving the rocket. Figure 25 shows the test stand with the rocket attached.

Figure 25: Test Stand used for Ignition Test

The single degree of freedom test stand is made from wood. The connector between the structure and the arm is a ball bearing joint so that the arm can be oscillated up and down around the VLR pitch axis. The rocket is tied to the eye hooks on the front and held in place by the leg rings as grips to the rocket. To test igniting the motor and verifying gimbal response, the software was modified to complete initialization and then immediately await a signal to ignite, after which a five second timer would commence before ignition. The signal to ignite the motor is sent when the critical enable pin is pulled.

This test was done utilizing the flight avionics. The ground station was also utilized to monitor the progression of the test and verify control responses as they occurred. The ignition circuit used is the same as the one used on the VLR and the thrust stand tests.

The first test conducted browned out the system which led to the selection of the current battery. The browning out occurred when the signal to ignite was sent and resulted in no data collection and no gimbal response during the motor burnout phase. The second round of tests with the new battery were successful. They showed the system being able to ignite the motor while maintaining power and connection to the ground station. The gimbal can also be seen as compensating for the orientation of the rocket during this test. Figure 26 shows the flame being directed to account for the VLR's orientation.

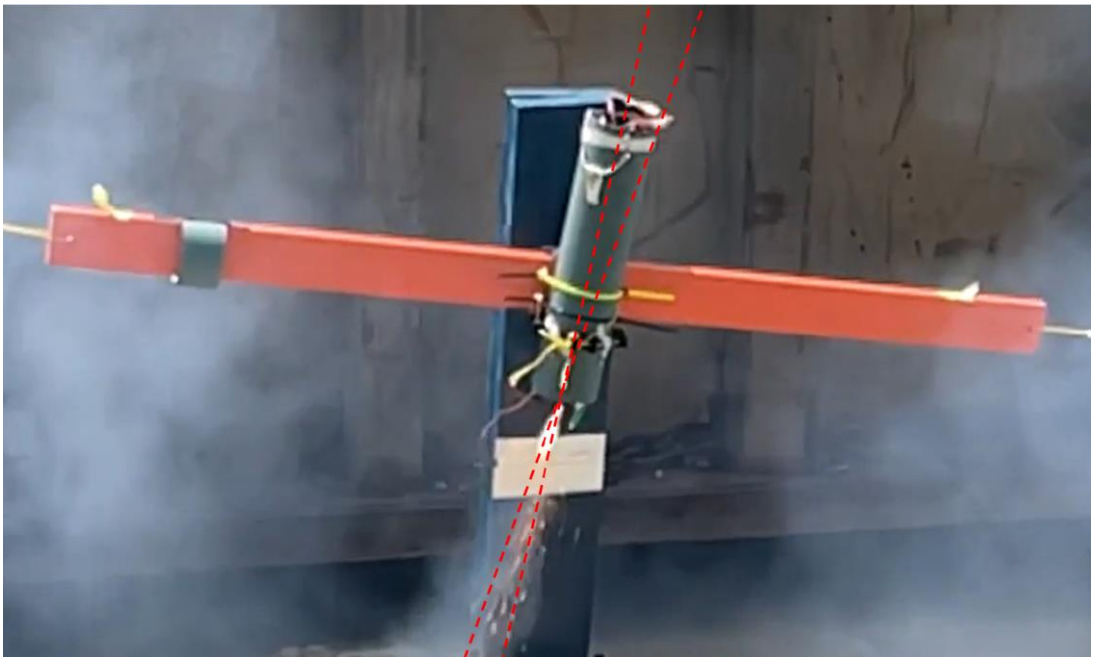

Figure 26: Gimbal Response Directing Flame

For the second ignition test, the ground station was able to communicate with the VLR for the entire duration and successfully stored data. Figure 27 shows the data collected from the thrust stand test.

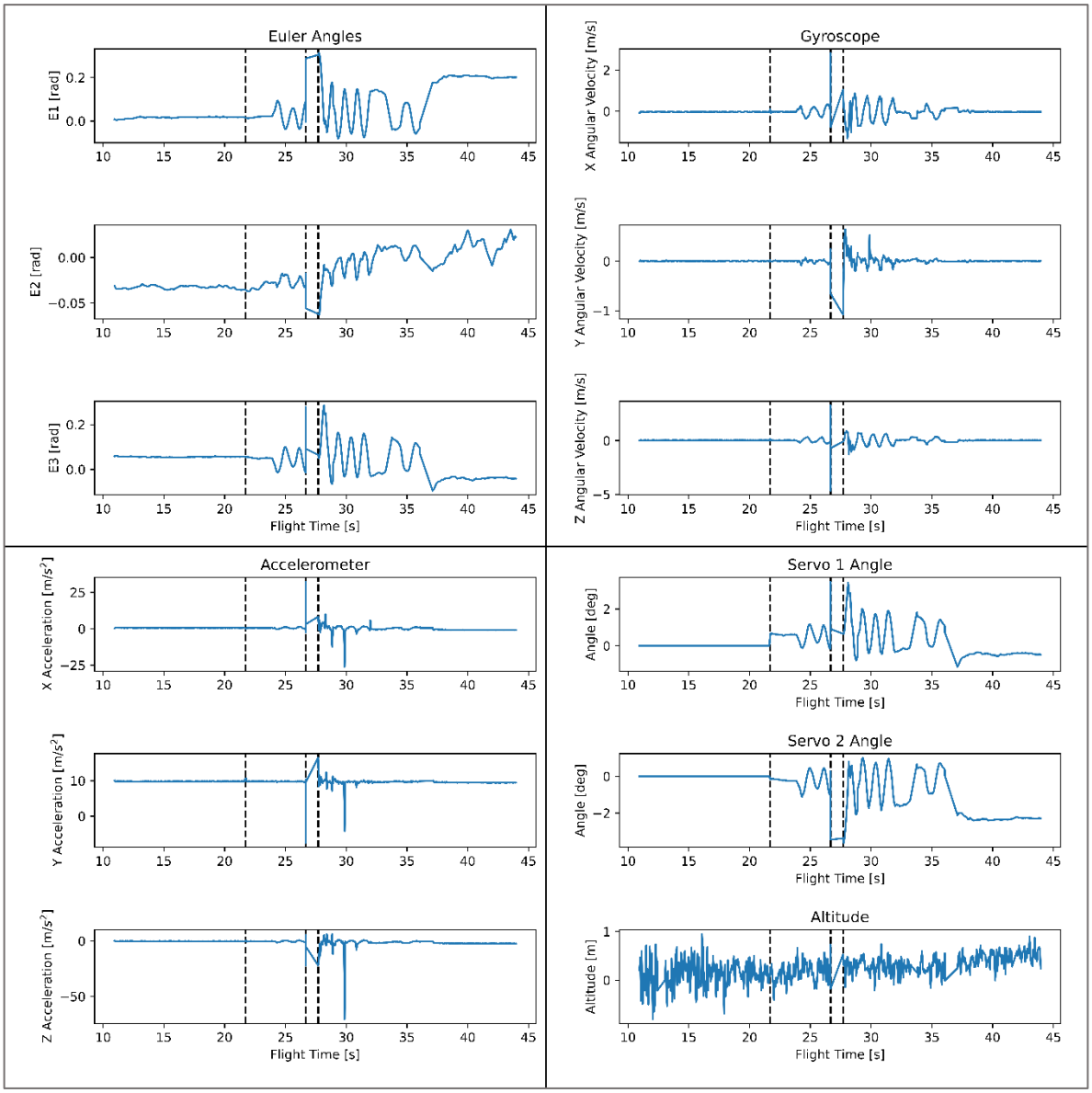

Figure 27: Data Collected from Thrust Stand Test

3.3 SOFTWARE VERIFICATION

3.3.1 MATLAB SIMULATION

Looking at the simulated VLR descent, there are several performance parameters that need to be selected for a successful landing. The MATLAB simulator incorporates these parameters, a kinematics integrator, and gimbal control law. For every time step of the simulated free fall, the software calculates VLR position, velocity, acceleration, rotation angles, angular rate, angular acceleration, aerodynamic forces, force from the rocket motor, resultant torque on the rocket body, and gimbal servo angles from the control law. Throughout this project, the simulation evolved into a high-fidelity simulation to provide an accurate projection of what a successful rocket landing looks like.

The Aerodynamic Forces Simulator component of the MATLAB simulator uses the geometric parameters of the rocket, as well as the information regarding airspeed and wind, to find the effect that the aerodynamic forces have on the body. The simulation then extracts forces and torque vectors from this which are used in calculating the acceleration of the rocket in the simulation, to be use in the kinematics integration.

The attitude simulator portion of the MATLAB simulation handles the calculation of the VLR attitude quaternion at each simulated time step. Because of complications that arise from using Euler angles leading to a gimbal lock, quaternion integration is used in this simulation. Using the torque data, angular rates, and angular positions, this attitude simulator is able to calculate the vehicle orientation. Figure 28 shows the output of a successful simulation run.

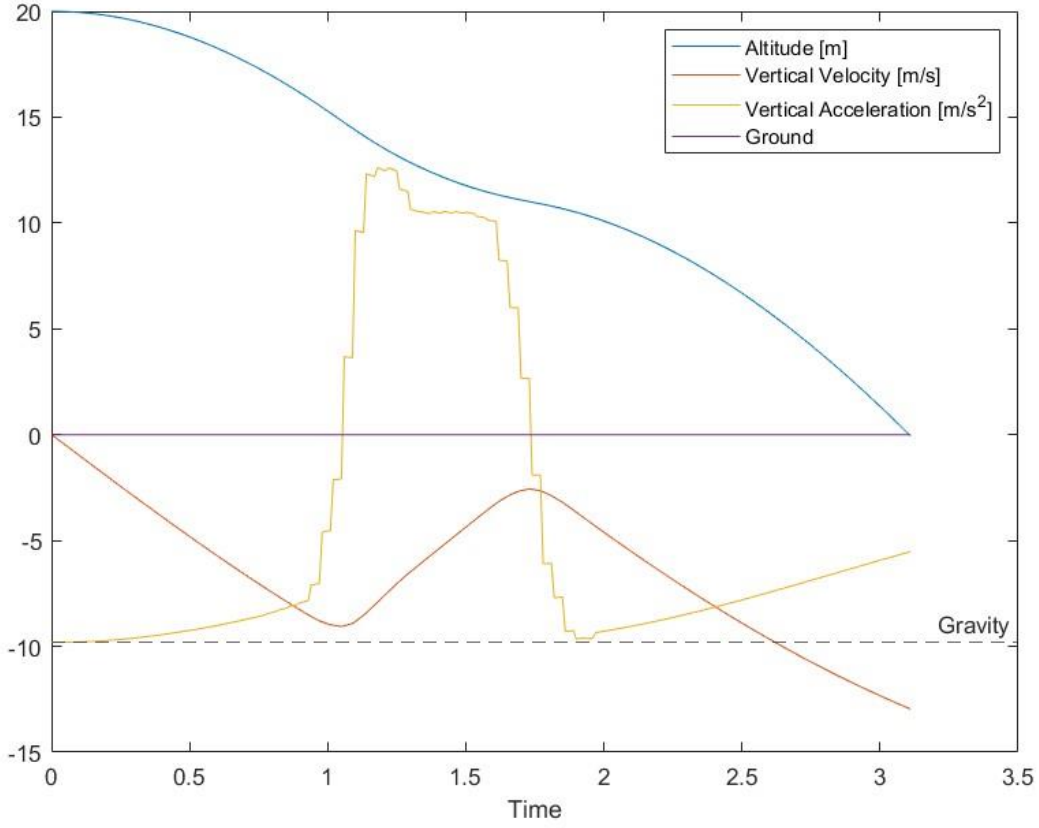

Figure 28: Data from Simulated Fall

3.3.2 CLOSED-LOOP TEST

To verify the VLR's software and its ability to land with sensor noise, a closed loop test was conducted. This was set up to feed computed data from the simulation to the VLR avionics package, which would take that data, add the noise of real sensors to their simulated values, and compute a control to send back to the simulation to generate the next time step dataset. This closed loop relationship is shown in Figure 29.

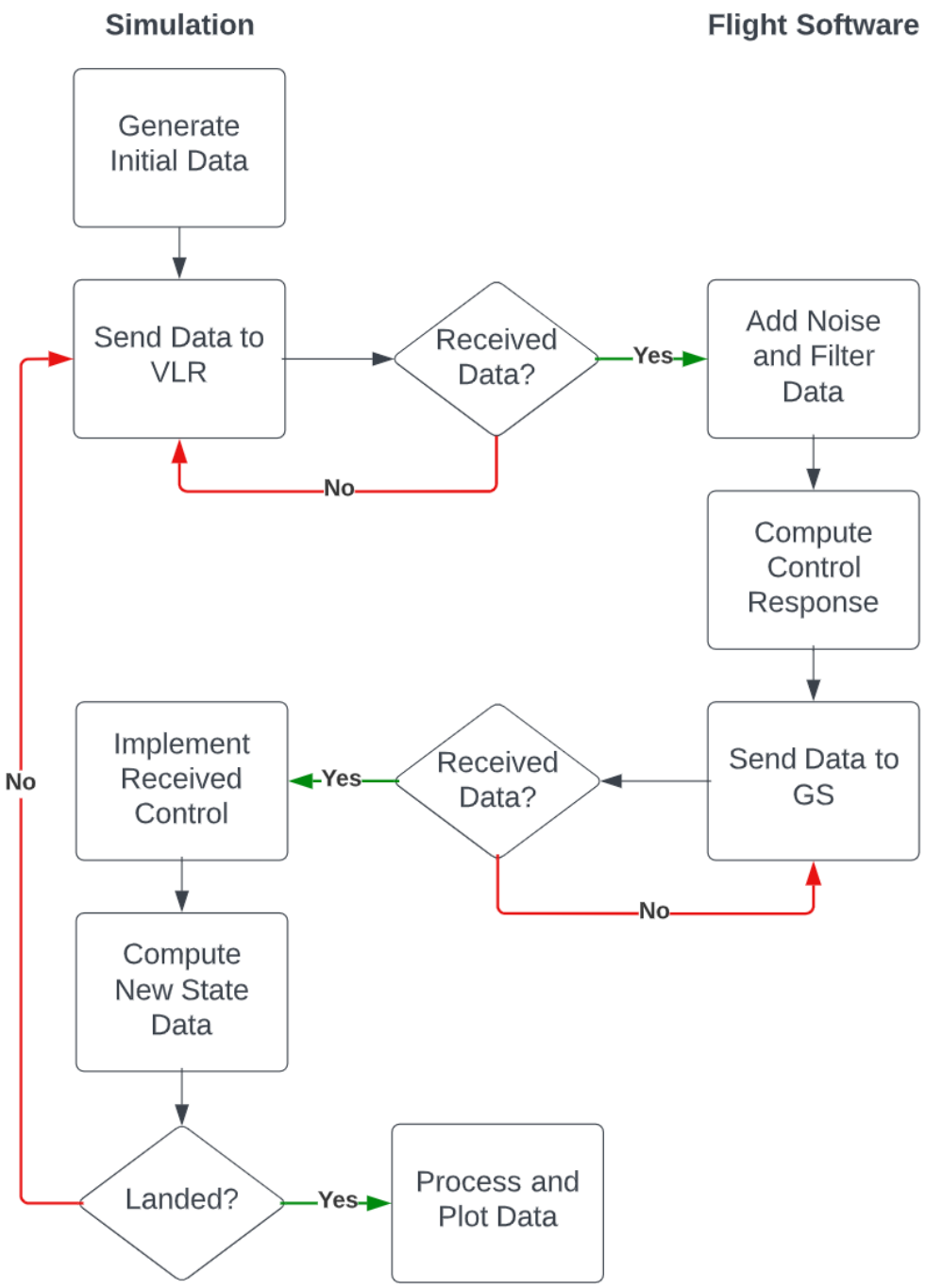

Figure 29: Closed Loop Test Diagram

To establish communication between the simulation and the VLR, a TCP/IP socket was utilized. The protocol sends a data packet from the simulator to the avionics and waits for a data packet to come back. If the data packet is the wrong size or not received in a prescribed period of time, the receiving end requests for the data to be sent again. The simulation provides the VLR with the time, orientation data, accelerometer readings, gyroscope readings, magnetometer readings, and altitude. The VLR then reads its sensors while the Raspberry Pi system is stationary on a table and adds the noise to the sensor readings. The noise was added to the data provided by the simulation and filtered, and a control was computed. The VLR then sent the angles and orientation data back to the simulation.

This process allowed for the continuous transfer of data and iterated through a simulated flight. The result of the test was that the VLR's software worked as expected and the filter used on the data was sufficient to maintain an accurate track of VLR orientation. This was found by comparing the data from the simulation with the data from the closed loop test under the same flight conditions. Figure 30 shows the output of the simulation without noise as well as the closed loop test which simulated a descent with noise.

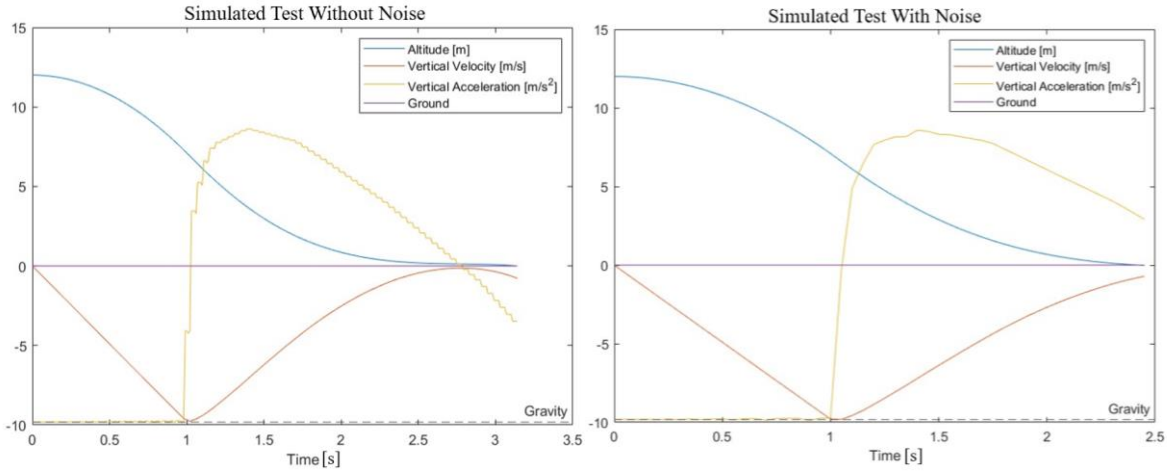

Figure 30: Data from Simulation without Noise (left) and Data from Closed Loop Test Simulation with Noise (right)

3.4 STRUCTURE VERIFICATION

To test the procedure for a powered drop and to verify the aerodynamics of the rocket and strength of the landing legs, a series of unpowered drop tests were conducted. The aim of these tests was to lift a test article of equivalent size and shape up to the desired drop height and to release it. This allowed the Drone Operator to practice flying before the powered flight and also allowed the team to observe an unpowered descent. In addition, this tested the tether, separation mechanism (pin puller), and Roll Inhibitor.

3.4.1 DROP TEST SERIES ONE

The team manufactured four drop test articles. The first two articles did not have the leg assembly attached, the third article had a set of rigidly attached sacrificial legs, and the fourth article had a leg assembly with crushable structures. The intention behind the first two drop articles was to validate the stability of the rocket before the legs were attached as they

dramatically increase the drag on the bottom of the rocket. After verifying the stability, the drop articles with legs were tested.

For each test, inside the VLR body was a simplified avionics package. This included a Teensy, a nine degree of freedom inertial measurement unit, and a barometer. The software was configured to start collecting data upon startup. It then saves and stores the data for later analysis. Each drop article was ballasted up with two masses to 940 g, the target weight of the flight VLR with redesigned structures. Each test article was labeled on its exterior for easy visual orientation identification.

On the test launch day, the winds were four mph with gusts up to five mph. The first two drop articles were of the rocket body with no legs. Figure 31 shows the drop article configuration for these two tests. The ballast masses were located on the bottom of the rocket and held in place by the avionics above and the bottom plate below on the drop article.

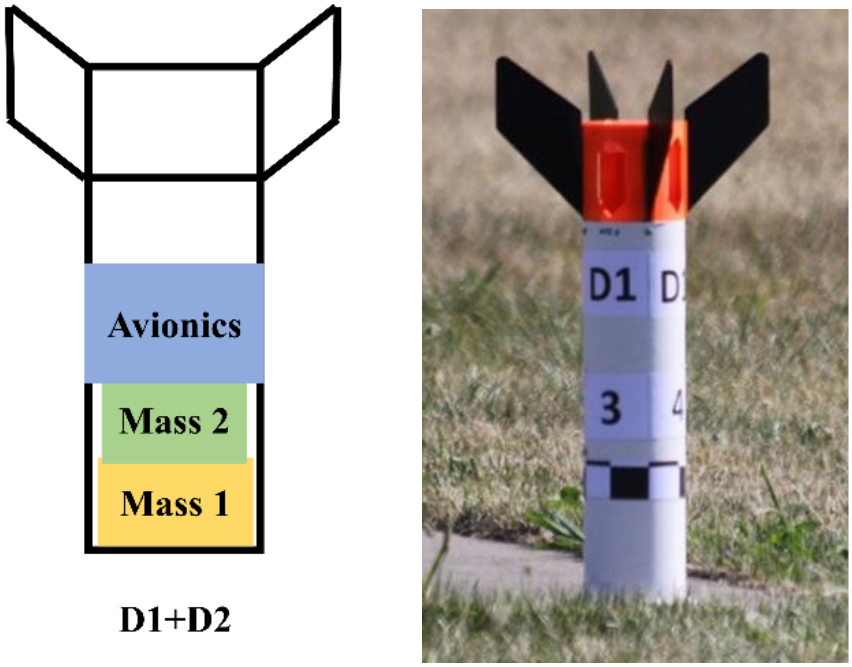

Figure 31: Drop Test Articles 1 and 2

The first drop article was lifted to 21 meters. The Drone Operator stabilized the platform and waited for the drop article to be nearly stationary prior to release. Drop article 1 experienced a stable release and descent to the ground. Figure 32 shows the drop article upright immediately before impact.

Figure 32: Drop Test Article 1 Before Impact

The drop test article landed with a significant impact on the ground. One fin broke and the avionics mount inside was broken. Due to the damage to the avionics and the battery, data was not collected, and the avionics were unable to be utilized to collect data on any of the other drop tests performed on this day. The landing orientation is shown in Figure 33.

Figure 33: Drop Test Article 1 Landing

After verifying the rocket structure without the legs was aerodynamically stable, the rigid leg assembly was added to observe how it influenced the VLR's aerodynamics. This article is pictured in Figure 34.

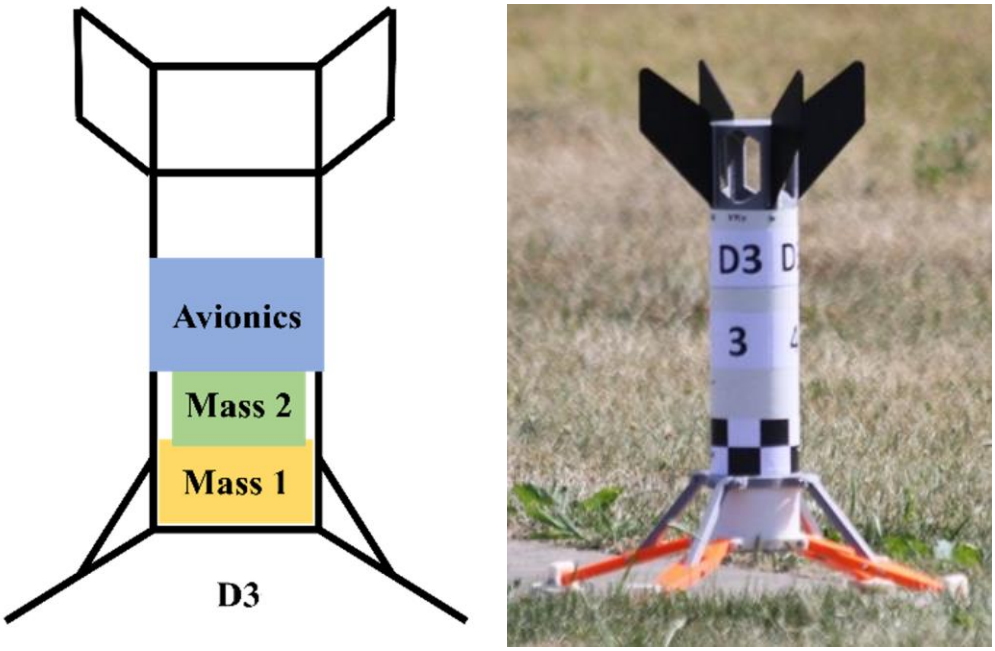

Figure 34: Drop Test Article 3

With the addition of the legs, a slight pitch oscillation was observed during the descent, but the design ultimately was found to be passively stable as it maintained a vertical orientation to the ground. Figure 35 shows the vertical orientation of D3 during the descent.

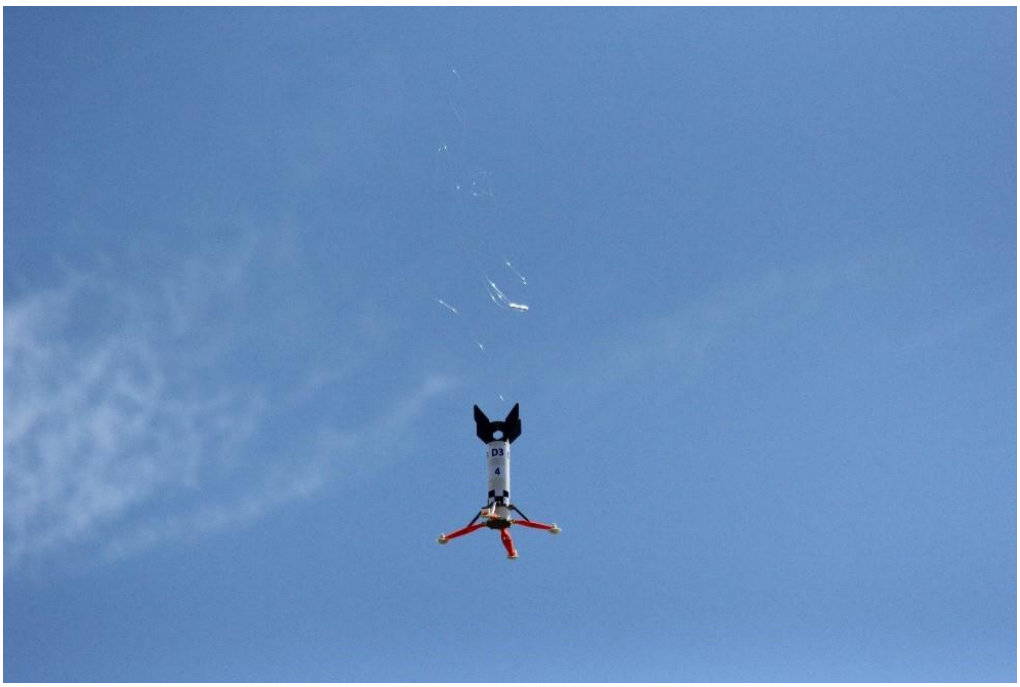

Figure 35: Drop Test Article 3 During Descent

After seeing the stability of the third article and the vertical impact, the next test article was equipped with crushable structure landing gear to see how the leg assembly would handle a drop from the specified 21 meters release height. The fourth article is shown in Figure 36. The unpowered test article landed upright before taking a small hop and falling over on its side on slightly inclined ground. The landing legs were intact, with the only slight damage observed to a fin at the top.

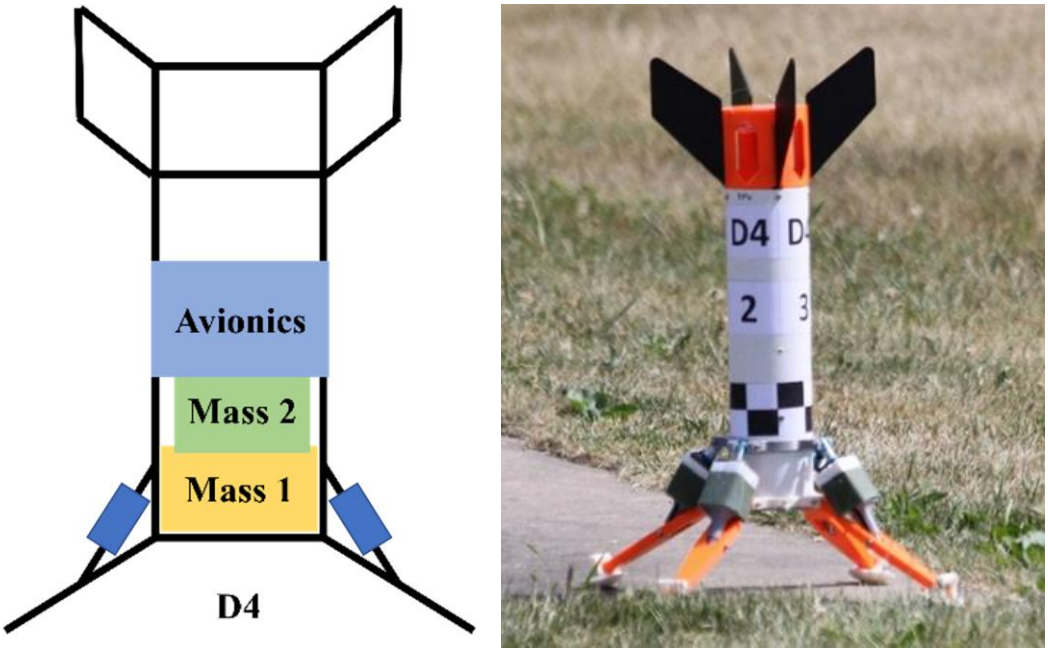

Figure 36: Drop Test Article 4

Figure 37 shows the landed orientation of the drop test article. The floral foam was completely crushed while the white foam was still intact as expected. From this test it was determined that the test article drag was apparently much higher than had been modeled in the MATLIB simulation, resulting in a much lower touchdown velocity than had been anticipated for an unpowered descent. Subsequently, performance requirements for a rocket motor for future drop tests was reconsidered and lowered to use a Quest D20-6W motor [20].

Figure 37: Drop Test Article 4 Landing

3.4.2 DROP TEST SERIES 2

Following the successes from the first set of drop tests, a second round of tests was conducted. The purpose of the second round was to repeat the same drops with working simplified avionics inside since the first series of tests were unable to collect descent data. Two test articles with both the fin and crushable leg assemblies were prepared for flight. This series of drop tests followed the same procedure as the first series with one addition: a target landing pad was placed in the field for the Drone Operator to line up over for consistent releases.

On launch day, the winds were five mph gusting to six mph. The first drop test used the test vehicle shown in Figure 38. The article was carried to a release height of 23 meters centered over the landing pad before release. As expected based on the results of the first round of drop tests, the descent was stable with minimal pitch oscillations. The article landed vertically but tipped over after touching down without damage to the VLR. A second test of the same configuration stuck the landing and did not tip over. Descent performance data was collected

from both tests and used to further refine the MATLAB descent simulation for future performance parameter tweaking.

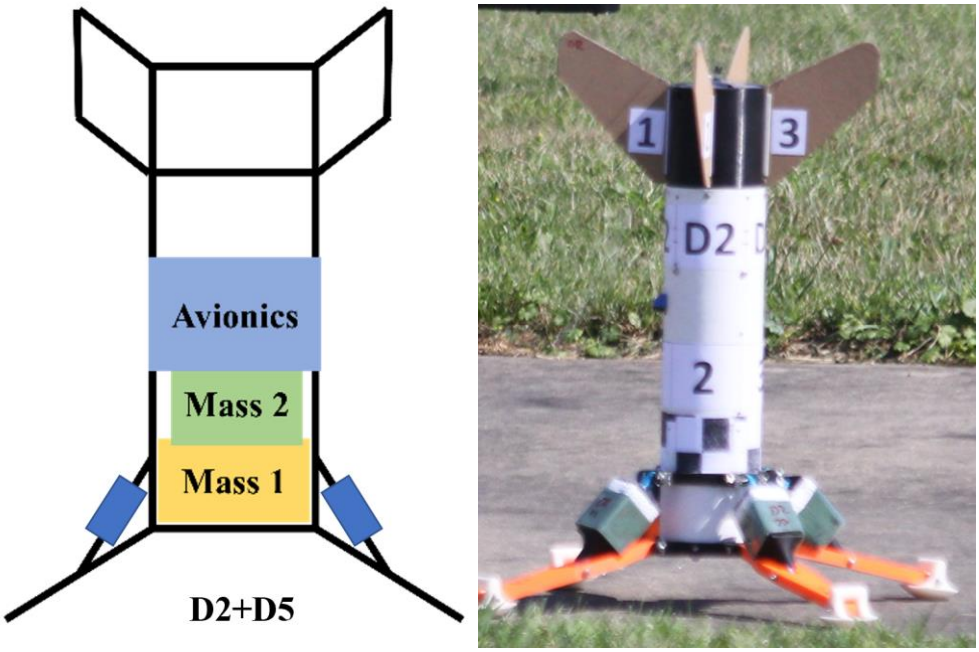

Figure 38: Drop Test Article 2

3.5 MODE PROGRESSION TEST

To test the procedure for a powered drop and to verify the mode progression of the software and retain connection with the ground station during operations, a mode test was conducted. To verify the progression of the modes, the rocket needed to be lifted by the UAV to the release height and brought back down. To do this, a flight ready article was made with all avionics and structures aside from the crushable foam and fins as this article was not going to be dropped.

As the intention was to verify the flight software, the goal was to modify it as little as possible for this test. However, as the rocket would not be dropped and no motor would ignite, there were two modifications: 1.) The condition to switch to the released mode only needed to

see a manual input to proceed, and 2.) No signal to ignite was sent. The plan was to lift the rocket up to the release height and wait until the rocket was stabilized. From there, the manual mode change command was sent from the ground station to tell it to progress to the release mode. This manual input is present in the final flight software, however, it usually is one of two conditions to progress to the released mode, with the second being the critical enable pin being pulled. In this test, the manual input moved the software to the released mode directly, at which point the UAV would then begin lowering the rocket back to the ground. Figure 39 shows the mode test article attached to the UAV.

Figure 39: Mode Test Article

This test was done utilizing all flight avionics and the ground station to monitor the progression of the test and verify control responses as they occurred as well as verify the ability to maintain connection with the rocket during the flight.

The mode test was conducted successfully, verifying the software's ability to step through the various modes. This test also verified the connection to the local Wi-Fi field router. Figure 40 shows the data saved from the ground station which is transmitted and collected at a lower rate than that recorded onboard the VLR. Figure 41 shows the data saved on the Raspberry Pi. The vertical lines on the images denote mode changes. Note that the ground station image has one less line between 100 and 125 seconds. This is due to the slow update rate of the ground station and the fast mode progression. Once released mode is reached, it progressed to ignition mode after half a second and then immediately to descent mode, with the ground station missing the ignition mode as the software progressed too quickly to transmit data while in that mode.

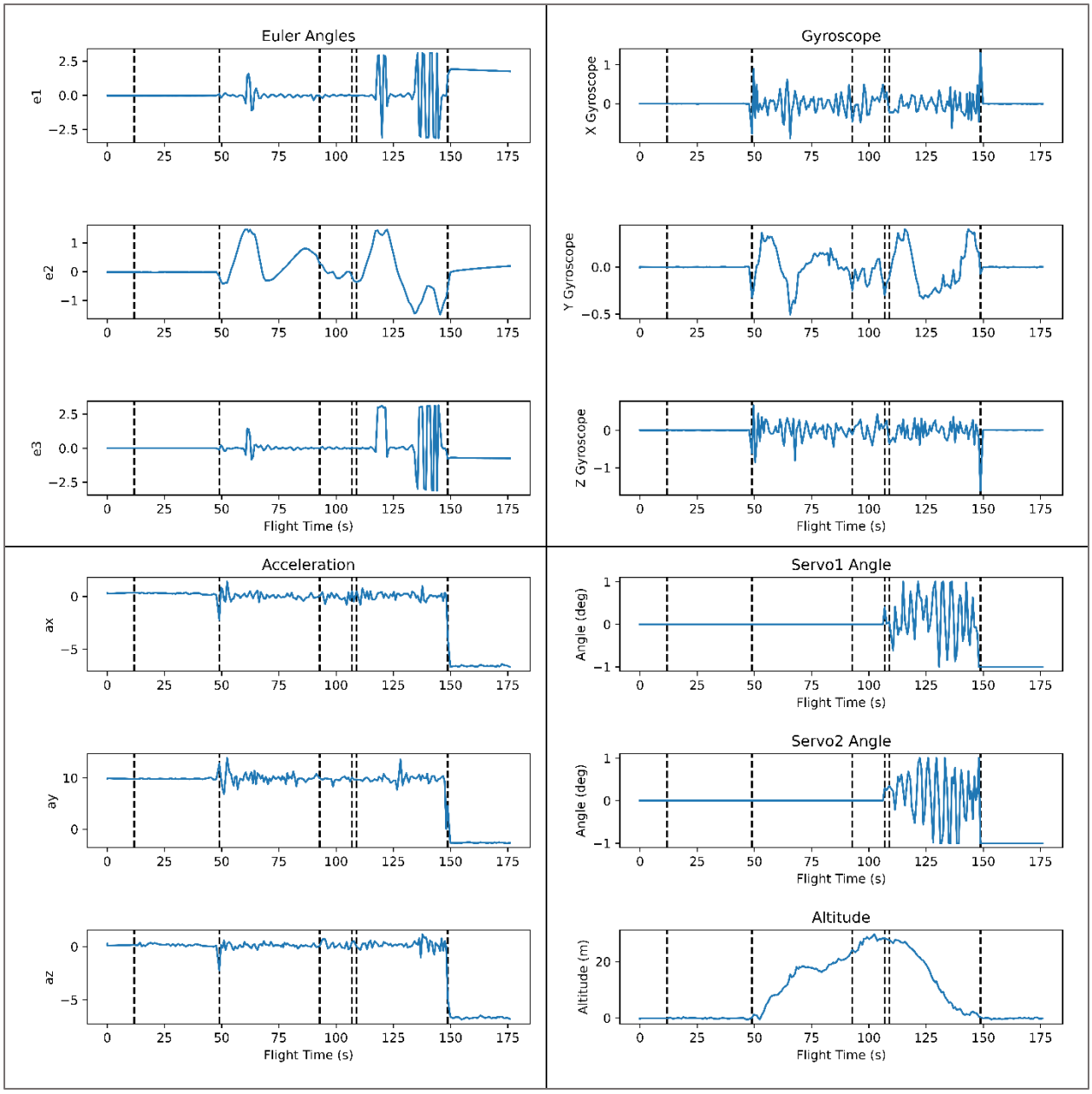

Figure 40: Ground Station Data

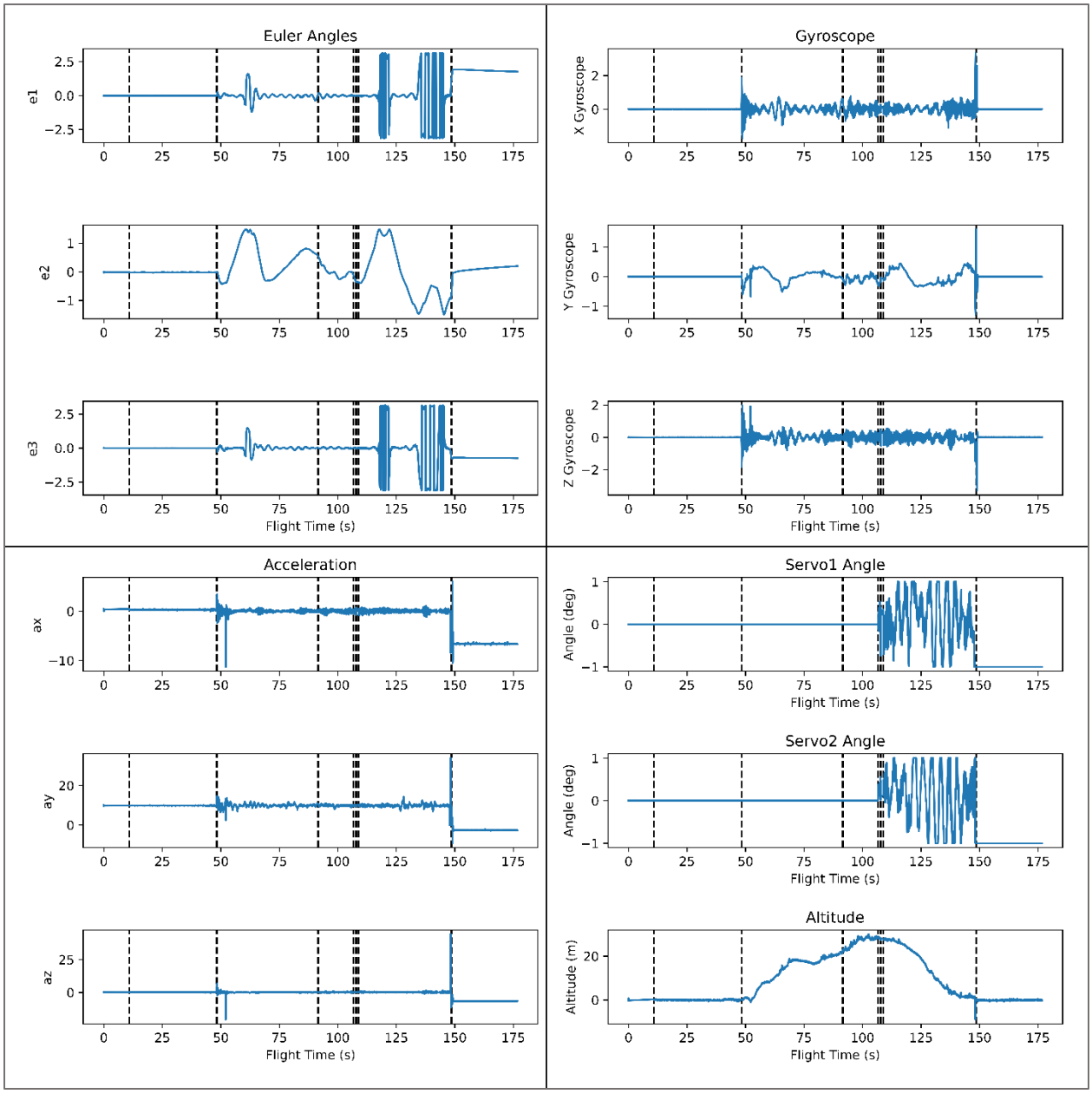

Figure 41: Raspberry PI Data from Mode Test

3.6 POWERED FLIGHT TEST RESULTS

To prepare for the powered flight test, a series of verification tests were conducted. A simulation had been created to predict the VLR's response and to find optimal flight parameters. The motor's thrust output and performance had been tested and verified and fed back into the simulation to refine parameters and performance predictions. A closed loop test was conducted

to examine the effect sensor noise would have on the rocket and to verify even in its presence, that the VLR could successfully land. A thrust test stand was created and tested on to verify that the avionics and power could ignite the motor and maintain control over the gimbal while remaining powered and in contact with the ground station. A mode verification test was conducted to verify the software's capability of stepping through the different modes of flight and to ensure data collection and unhindered connection with the ground station. Finally, a series of drop tests were conducted to verify the passive stability of the rocket and to verify the landing legs' ability to accept and disperse energy of landing.

This series of tests let the team move forward with the powered test as every system had been tested and verified and approved for launch.

3.6.1 POWERED DROP

The first powered drop was conducted on the same day of the second round of passive drop tests. The day of launch had a wind speed of five mph with gusts up to six mph, with clear visibility. Figure 42 shows the configuration of the powered flight test article.

Figure 42: Flight Test Article D6

For this test, the flight software was configured to limit the gimbal response to one degree of rotation in each axis to mitigate flight excursions in the event of gimbal lock.

The VLR was released from the UAV at an altitude of 20 meters and was observed descending vertically with the same previously observed small oscillatory motion in pitch. Figure 43 shows the VLR at the time of ignition.

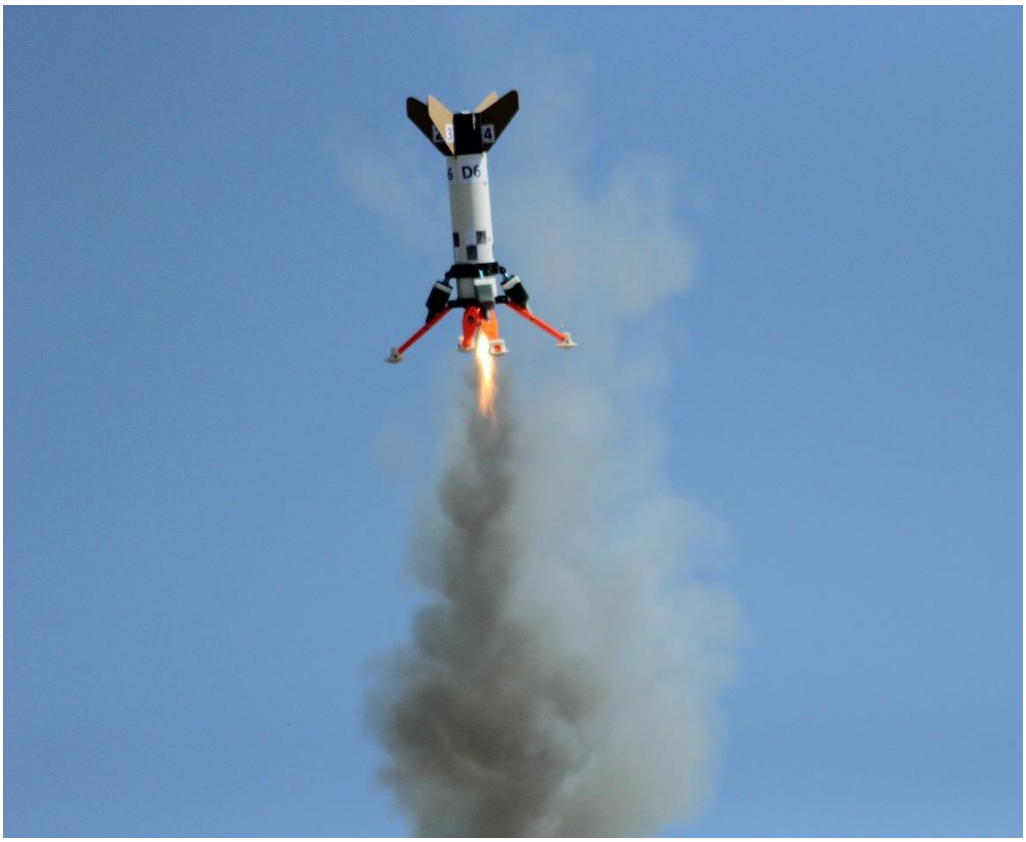

Figure 43: D6 at Ignition

The VLR ignited as expected about one second after release, and rapidly decelerated the vehicle. With the fins no longer stabilizing the vehicle, the gimbaled rocket motor over-controlled the pitch of the vehicle and turned it on its side. Figure 44 shows the flight performance data collected from the time of release from the UAV to landing. Looking at the control response in the bottom right, the servos quickly went to the extremes to correct for the

tipping rocket. As the vehicle exceeded the predetermined angle of 45-degrees, the software commanded safe mode and set the commanded servo angles to zero degrees. One thing to note is that the VLR was not tracking height correctly throughout the flight. It tracked a drop height of 14 meters. This is likely due to the barometer not sensing free stream pressure and lagging behind as it is inside the rocket with all the other avionics.

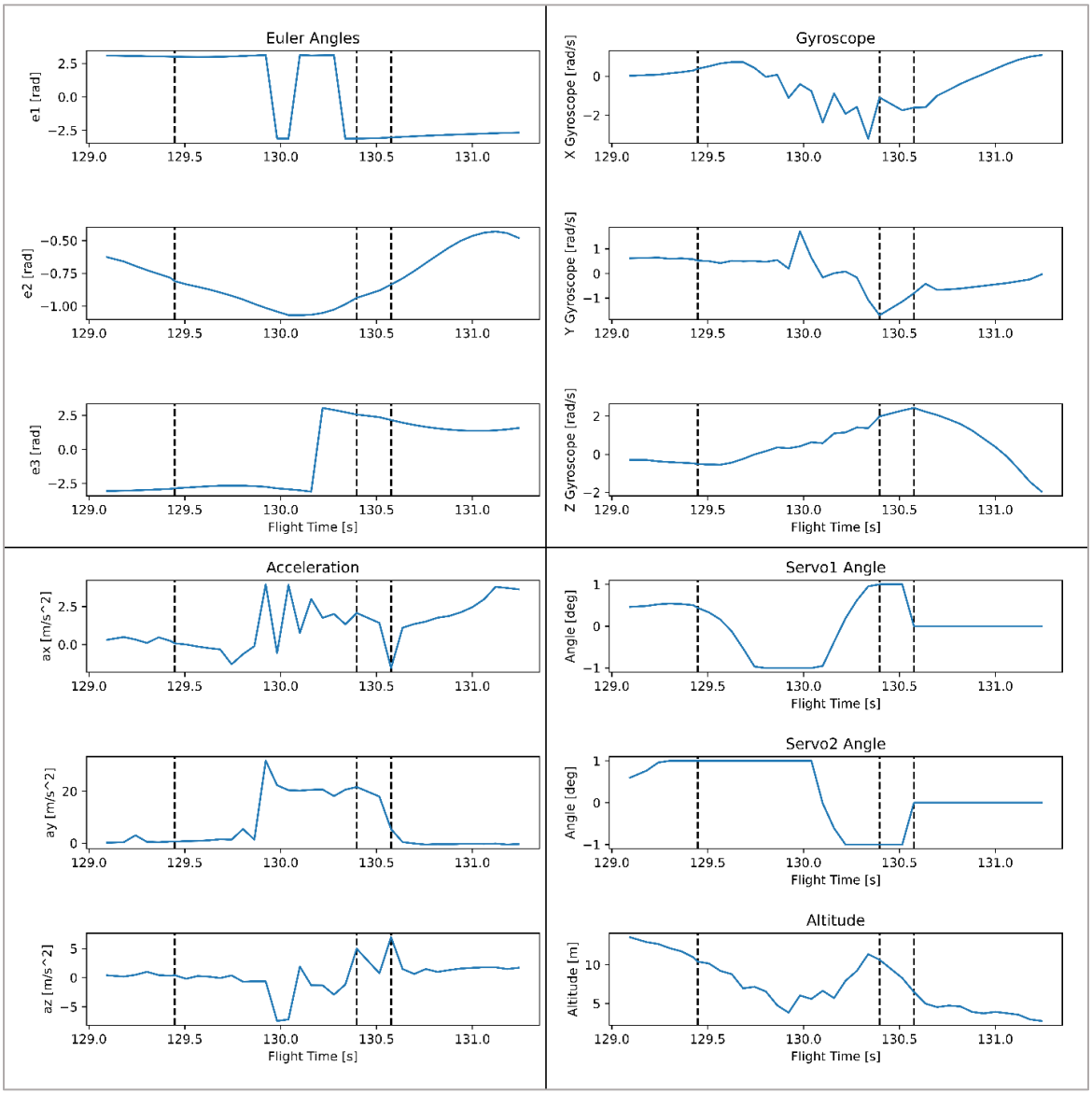

Figure 44: D6 Descent Data

For the next set of tests, the control response gains will be retuned. The gains for this drop were a position gain of 0.4 and a rate gain of 0.01. This heavily favored correcting for a position offset from vertical. The motor also burned out while the rocket was still midway through the descent and can be biased lower. Increasing the ignition delay will also allow the fins to provide more control at a higher velocity during the initial ignition pulse. The team is also looking into GPS capabilities to better monitor the rocket's height and position.

CHAPTER 4: CONCLUSION

4.1 OBJECTIVE COMPLETION

The main objective of this thesis was to design a VLR that student teams could select performance parameters for and participate in a challenge competition while learning from the experience. This objective was successfully met.

The team was able to accomplish testing and validation of each individual system. Future work revolves around continued tuning the launch parameters, motor selection, and control response. The validation process included the following: A simulation to predict the flight trajectory and outcome given the control response that would accept real data to better represent the true flight; a thrust test to verify motor thrust output; a closed loop test to verify the flight software; a test stand verification of the ability to ignite a motor and maintain operations; a mode test to verify the software's ability to track the descent and communicate with the ground station; and drop tests to verify passive stability and landing legs.

4.2 FUTURE WORK

This project is continuously evolving and improving over time with upgraded simulation capabilities and additional drop tests planned. As a result of the flight tests that were conducted, several changes have been or are being made to the design for future evaluation. The following changes occurred between the mode test and the hot fire test that have not yet been discussed herein.

The structure of the rocket body was changed from Blue Tube to a white cardboard tube. This was done to conserve mass after preliminary tests showed that the strength of the Blue Tube was not needed and that the white cardboard would be sufficient.

The avionics bay has been redesigned to have the battery, avionics, and gimbal all attached. This is done by having three structures that combine for ease of assembly. This provides the user with the capability to remove all interior components easily and together rather than having to unscrew and disassemble each part. This also minimizes risks associated with assembling components that are connected through the electronics.

The fin cap has been remodeled to have a hole at the top that the tether to the UAV can be threaded through, rather than attaching a tube inside the cap.

The fin shape and material has been changed. The fins no longer have the T slot into the cap, rather they slide directly into a slot in the cap and are epoxied in place. They are now made from a stiff cardboard. This design choice comes from the repeated breaking of 3D printed fins. The stiff cardboard is stronger than the PLA and is easier to manufacture in quantity.

The motor has been changed to a smaller Quest D20-6W motor. Drop test results demonstrated that the leg drag was much higher than previously modelled, resulting in much lower unpowered landing velocities. Test results indicate that the E20W-7 is significantly stronger than required and that a smaller motor will be sufficient.

REFERENCES

[1] "Spacelab Illinois," [Online]. Available: https://spacelab.web.illinois.edu/.

[2] "The Delta Clipper Experimental: Flight Testing Archive," 26 December 2012. [Online]. Available: https://www.hq.nasa.gov/pao/History/x-33/dc-xa.htm.

[3] D. Sorid, "Roton Tester Flies Down in the Desert," 19 October 1999. [Online]. Available: https://web.archive.org/web/20040612024546/http://space.com/missionlaunches/launches/roton_thirdflight.html.

[4] Art of Engineering, *How SpaceX Lands Rockets with Astonishing Accuracy,* 2020.

[5] "ROCKETLAB," [Online]. Available: https://www.rocketlabusa.com/launch/neutron/.

[6] "Blue Origin," [Online]. Available: https://www.blueorigin.com/new-shepard/.

[7] "Blue Origin," [Online]. Available: https://www.blueorigin.com/new-glenn/.

[8] "Illinois X Space Technologies Academy," [Online]. Available: http://illinoisx.niu.edu/.

[9] "AeroTech E20W," thrustcurve.org, [Online]. Available: https://www.thrustcurve.org/motors/AeroTech/E20W/.

[10] R. Pi, "Raspberry Pi 3 Model B+," [Online]. Available: https://www.raspberrypi.com/products/raspberry-pi-3-model-b-plus/.

[11] "Navio2," Emlid, [Online]. Available: https://navio2.emlid.com/.

[12] InvenSense, "MPU-9250 Product Specification Revision 1.1," [Online]. Available: https://invensense.tdk.com/wp-content/uploads/2015/02/PS-MPU-9250A-01-v1.1.pdf.

[13] T. Connectivity, "MS5611-01BA03," [Online]. Available: https://www.amsys-sensor.com/downloads/data/MS5611-01BA03-AMSYS-datasheet.pdf.

[14] "Aurelia X6 Standard," Aurelia Aerospace, [Online]. Available: https://aurelia-aerospace.com/product/aurelia-x6-standard/.

[15] Mario Garcia Revision, "Madgwick Orientation Filter," 2019-2022. [Online]. Available: https://ahrs.readthedocs.io/en/latest/filters/madgwick.html.

[16] A. J. L. H. R. V. Sebastion O. H. Madgwick, "Estimation of IMU and MARG orientation using a gradient descent algorithm," in *2011 IEEE International Conference on Rehabilitation Robotics*, 2011.

[17] "80/20," [Online]. Available: https://8020.net/.

[18] github, "HX711," [Online]. Available: https://github.com/bogde/HX711.

[19] R. Meier, "Roger Meier's Freeware," [Online]. Available: https://freeware.the-meiers.org/.

[20] A. Components, "QUEST Q-JET COMPOSITE MOTOR -D20-6W," [Online]. Available: https://www.apogeerockets.com/Rocket-Motors/Quest-Motors/Quest-Q-Jet-Composite-Motor-D20-6W#description.